The Journal of
Eukaryotic Microbiology

Published by the International Society of Protistologists

J. Eukaryot. Microbiol., ■■(■■), 2010 pp. 1–15

DOI: 10.1111/j.1550-7408.2010.00504.x

Tintinnophagus acutus n. g., n. sp. (Phylum Dinoflagellata), an Ectoparasite of the Ciliate *Tintinnopsis cylindrica* Daday 1887, and Its Relationship to *Duboscquodinium collini* Grassé 1952

D. WAYNE COATS,[a,1] SUNJU KIM,[a] TSVETAN R. BACHVAROFF,[a] SARA M. HANDY[b] and CHARLES F. DELWICHE[b]

[a]*Smithsonian Environmental Research Center, P. O. Box 28, Edgewater, Maryland 21037, and*
[b]*Cell Biology, and Molecular Genetics, University of Maryland, College Park, Maryland 20742*

ABSTRACT. The dinoflagellate *Tintinnophagus acutus* n. g., n. sp., an ectoparasite of the ciliate *Tintinnopsis cylindrica* Daday, superficially resembles *Duboscquodinium collini* Grassé, a parasite of *Eutintinnus fraknoii* Daday. Dinospores of *T. acutus* are small transparent cells having a sharply pointed episome, conspicuous eyespot, posteriorly positioned nucleus with condensed chromosomes, and rigid form that may be supported by delicate thecal plates. Dinospores attach to the host via a feeding tube, losing their flagella, sulcus, and girdle to become spherical or ovoid cells. The trophont of *T. acutus* feeds on the host for several days, increasing dramatically in size before undergoing sporogenesis. Successive generations of daughter sporocytes are encompassed in an outer membrane or cyst wall, a feature not evident in trophonts. *Tintinnophagus acutus* differs from *D. collini* in host species, absence of a second membrane surrounding pre-sporogenic stages, and failure to differentiate into a gonocyte and a trophocyte at the first sporogenic division. Phylogenetic analyses based on small subunit (SSU) ribosomal DNA (rDNA) sequences placed *T. acutus* and *D. collini* in the class Dinophyceae, with *T. acutus* aligned loosely with *Pfiesteria piscicida* and related species, including *Amyloodinium ocellatum*, a parasite of fish, and *Paulsenella vonstoschii*, a parasite of diatoms. *Dubosquodinium collini* nested in a clade composed of several *Scrippsiella* species and *Peridinium polonicum*. Tree construction using longer rDNA sequences (i.e. SSU through partial large subunit) strengthened the placement of *T. acutus* and *D. collini* within the Dinophyceae.

Key Words. Ciliate, dinoflagellate, parasite, taxonomy, tintinnids.

FRESHWATER and marine ciliates host a diverse array of parasitic organisms including bacteria, fungi, flagellates, and even other ciliates (Ball 1969). Few of these parasites have been brought into culture, and, thus, little is known about their biology, mode of transmission, or influence on host organisms. Even less is known about their prevalence in natural systems and their impact on host populations.

Among the better studied pathogens of marine ciliates are the parasitic dinoflagellates (Cachon and Cachon 1987), of which three genera, *Amoebophrya*, *Duboscquella*, and *Duboscquodinium*, include species categorized as intracellular parasites of tintinnids, aloricate choreotrichs, oligotrichs, prorodontids, and apostomes (Cachon 1964). Several other dinoflagellate genera act as extracellular parasites of protists, invertebrates, and vertebrates, but none of their species is known to infect ciliates. The three genera that infect ciliates are placed in the Syndinea, a subdivision of dinoflagellates whose members are endoparasites (i.e. intracellular, or in host body fluids) having a flagellate dinospore stage in their life cycle and possessing histones in their nucleus (Fensome et al. 1993). Small subunit (SSU) ribosomal DNA (rDNA) sequences place *Amoebophrya*, *Duboscquella*, and other syndinians with the Group I and Group II marine alveolates, forming basal lineages to the Dinokaryota (Guillou et al. 2008; Harada, Ohtsuka, and Horiguchi 2007; Skovgaard, Menese, and Angélico 2009; Skovgaard et al. 2005).

The life cycles of dinoflagellates parasitic on ciliates encompass a bi-flagellated infective stage, the dinospore, that may actively penetrate the host cell membrane (e.g. *Amoebophrya*) or be ingested by the host (e.g. *Duboscquella*) (Cachon 1964). Once inside the host, the parasite grows into a large trophont that occupies much of the host cytoplasm. In *Amoebophrya*, the trophont is multinucleate, ruptures through the host cell at maturity, and then completes cytokinesis to liberate numerous dinospores. *Duboscquella*, on the other hand, remains uninucleate as a trophont, ruptures through the host cell membrane ingesting part, or all, of the remaining host cell, then undergoes rapid sequential nuclear and cytoplasmic divisions to produce dinospores. Far less is known about the life cycle of *Duboscquodinium*, as species of that genus have not been studied since the very brief original descriptions provided by Grassé (1952 in Chatton 1952).

Duboscquodinium collini Grassé, a parasite of *Eutintinnus fraknoii*, is the type species for the genus and was described along with *Duboscquodinium kofoidi* Grassé, a parasite of *Tintinnopsis campanula*. Placement of *D. kofoidi* within the genus was provisional (designated as *Duboscquodinium* (?) *kofoidi*; Fig. 297 in Chatton 1952), as it exhibited an unusual ''rosace'' pattern during sporogenesis. Neither species was reported inside a host cell, or in a lorica that also contained a host organism. Thus, description of the two parasites relied exclusively on attributes of their post-feeding stage (= tomont) and sporogenesis, leaving uncertain whether the species are endoparasitic or ectoparasitic. Species of *Duboscquodinium* differ from those of *Duboscquella* and *Amoebophrya* by possessing a typical dinokaryon with moniliform chromosomes and by producing ''*Gymnodinium*-like,'' rather than ''*Oxyrrhis*-like'' dinospores (Chatton 1952). In addition, *D. collini* was reported to possess a double outer membrane.

Here we describe *Tintinnophagus acutus* n. g., n. sp., an ectoparasitic dinoflagellate that infects the tintinnid ciliate *Tintinnopsis cylindrica*. We also provide phylogenies based on SSU only and longer SSU through partial large subunit (LSU) rDNA sequences that places *T. acutus* within the Dinophyceae and aligned with the Pfiesteriaceae. Finally, we consider the implications of new observations for *D. collini* from *E. fraknoii* and review past reports of dinoflagellate parasites of tintinnids, offering comment regarding ambiguities in parasite life cycle, dinospore morphology, and nomenclature.

MATERIALS AND METHODS

Sampling protocol. *Tintinnopsis cylindrica* parasitized by *T. acutus* n. g., n. sp. was collected from the Chesapeake Bay during cruises in fall to spring of 1989–1991 and from shore in January, February, and December of 2008 and 2009. Cruise stations yielding infected *T. cylindrica* were in the mesohaline portion of the Bay (Fig. 1): Stations 858 (38°58′N; 76°23′W), 845

Corresponding Author: Sunju Kim, Smithsonian Environmental Research Center, P. O. Box 28, Edgewater, Maryland 21037, USA—Telephone number: +1 443 482 2446; FAX number: +1 443 482 2380; e-mail: kimsu@si.edu

[1]Present Address: US FDA Center for Food Safety and Applied Nutrition, 5100 Paint Branch Parkway, College Park, Maryland 20740, USA.

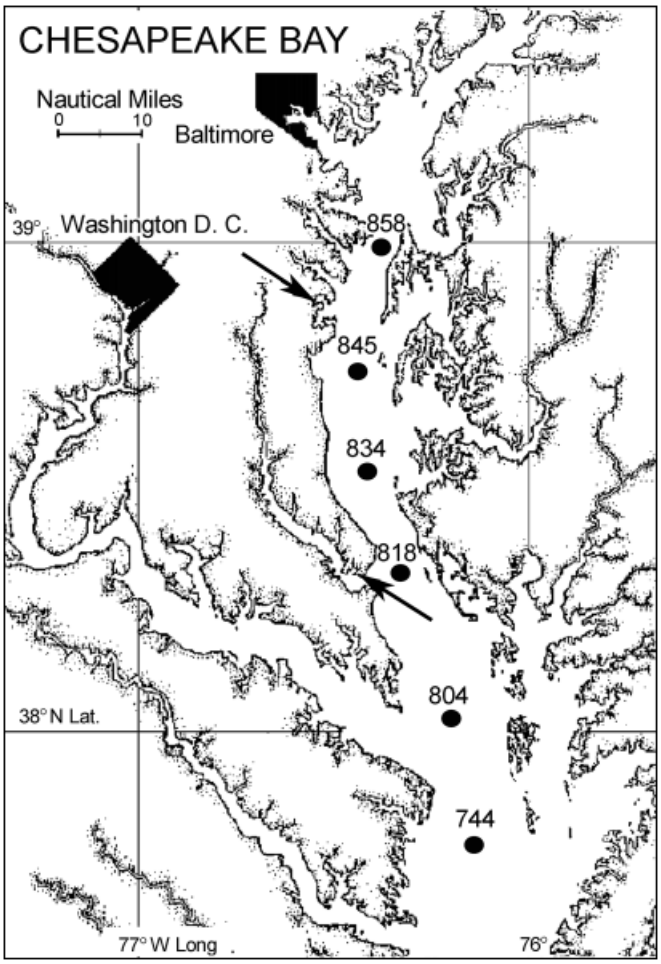

Fig. **1.** Sampling sites where *Tintinnophagus acutus* n. g., n. sp. was collected from Chesapeake Bay. Filled circles are stations sampled from ship in 1989–1991. Arrows indicate stations sampled from shore in 2008 and 2009.

(38°45′N; 76°26′W), 834 (38°34′N; 76°26′W), 818 (38°18′N; 76°17′W), 804 (38°04′N; 76°13′W), and 744 (37°44′N; 76°11′W). Sampling at each station consisted of 5–10 depth discrete samples taken between the surface and bottom using a Sea-Bird conductivity-temperature-depth profiling system with 10-L Niskin-bottle rosette (Sea-Bird Electronics Inc., Bellevue, WA) and a vertical plankton tow taken over the upper 10 m using a plankton net with a 25-cm opening and a 35-μm mesh (SEA-GEAR Corp., Melbourne, FL). Stations sampled from shore were located in the Rhode River and Patuxent River subestuaries of Chesapeake Bay (38°52′N, 76°32′W; 38°19′N, 76°27′W, respectively; Fig. 1). Surface plankton tows (35 μm net as above) and whole water samples were collected from shore, with temperature and salinity measured using hand-held thermometer and refractometer. Samples from the Rhode River and Patuxent River were placed in coolers with ice and within 1 h transported to the lab for examination.

Eutintinnus fraknoii loricae containing *D. collini* were obtained in a single plankton sample taken on September 10, 2009 from the Bay of Villefranche-sur-Mer, France (Station B of the Laboratoire de Océanographie de Villefranche: 43°41.10′N; 7°18.94′E). Specimens were collected from surface water using a 35-μm net (as above) and transported to the lab for examination.

In vivo observation of parasite morphology and development. In vivo morphology and development of *T. acutus* n. g., n. sp. was examined using specimens obtained in winter and spring of 1991. To follow parasite development and assess generation time, *T. cylindrica* infected by *T. acutus* measuring 5–10 μm in diameter were isolated by micropipette, washed several times in filtered site water (0.45 μm filter, Millipore Corp., Billerica, MA), and incubated in humidity chambers at ambient water temperature (6 °C and 8 °C) following methods of Coats (1988). Specimens were examined (400–1,000X) at 6–12 h intervals using a Zeiss WL microscope or Zeiss Axioscope with epifluorescence capabilities (Zeiss 09 filter set: 450–490 nm excitation, 510 nm barrier, 520 nm emission) to determine parasite size, shape, and number of dinospores emerging from host loricae (Carl Zeiss Inc., Thornwood, NY). The time from isolation of specimens to the first indication of sporogenesis was taken as the duration of the vegetative growth phase, while the time from the first indication of cell division to emergence of one or more dinospores from the host lorica was taken as the duration of sporogenesis. Parasite generation time was calculated as the sum of the duration of the vegetative growth phase and sporogenesis.

Additional observations of trophonts, sporocytes, and dinospores of *T. acutus* were made using wet mount preparations of specimens collected in 2008 and 2009. To obtain dinospores, infected *T. cylindrica* were isolated from plankton samples using micropipettes, washed 6 times in 0.45 μm filtered site water, and transferred to 24-well Falcon plates (Becton Dickinson & Co., Lincoln Park, NJ). Wells receiving 2 ml of filtered site water and 10–100 infected host cells were incubated at ambient water temperature (~ 7 °C) and allowed to produce dinospores over the following 2–5 d. Photographs and measurements of live specimens were obtained using a Zeiss Axiocam interfaced with a PC running Zeiss Axiovision software (Carl Zeiss Inc.).

Specimens of *D. collini* located in the lorica of *E. fraknoii* were viewed and photographed using an Olympus IX71 microscope equipped with DIC optics and a DP71 camera (Olympus France SAS, Rungis Cedex, France) or a Zeiss Axiovert 25 with epifluorescence capabilities (Zeiss 09 filter set: 450–490 nm excitation, 510 nm barrier, 520 nm emission). The camera was interfaced with a PC running Olympus BioCell image analysis software with scale calibration (Olympus France SAS). Measurements for specimens were obtained from digital images using Axiovision software.

Parasite cytology. Organisms present in 4 L of each Niskin-bottle sample were concentrated to 20 ml using 20-μm Nitex screening (Sterling Net & Twine Co. Inc., Montclair, NJ). Resulting concentrates and a portion of each net tow were preserved with modified Bouin's fixative (Coats and Heinbokel 1982) and processed by the Quantitative Protargol Staining (QPS) technique of Montagnes and Lynn (1993). For cytological observation of *T. acutus* dinospores, infected *T. cylindrica* were incubated in filtered site water as above, with emerging dinospores preserved in 2% (v/v) glutaraldehyde, 4% (v/v) formaldehyde, or 35% (v/v) methanol for direct examination and calcoflour staining (Dider et al. 1995; Eschbach et al. 2001; Fritz and Triemer 1985; Palacios and Marín 2008), or in modified Bouin's for QPS staining. Preserved and stained specimens were examined, photographed, and measured using a Zeiss Axioscope, Axiocam, and Axiovision software as above.

Scanning electron microscopy (SEM) of parasite dinospores. Dinospores of *T. acutus* obtained as above were processed for SEM following numerous protocols used in recent years to visualize thecal plates of lightly armored dinoflagellates. The protocols included ''membrane swelling'' techniques (Glasgow et al. 2001; Parrow et al. 2006), ''membrane stripping'' techniques (Mason et al. 2003; Steidinger et al. 1996), and various formulations of osmium and mercuric chloride (Hansen, Daugbjerg, and Henriksen 2007;

Moestrup, Hansen, and Daugbjerg 2008). Images provided in this manuscript are for specimens preserved in glutaraldehyde (2% [v/v] final concentration) and stored at 4 °C. Glutaraldehyde-fixed samples were concentrated onto 1 μm pore size, 13 μm diameter Nucleopore filters (Whatman Inc., Piscataway, NJ), rinsed 3 times in filtered site water, and post-fixed for 1 h in 1% (w/v) osmium tetroxide at salinity equivalent to site water (~ 15 psu). Following osmium, specimens were rinsed 3 times in distilled water, dehydrated in a graded ethanol series, dried using a Denton DCP-1 critical point apparatus (Denton Vacuum, LLC, Moorestown, NJ), coated with gold-palladium alloy, and examined on an AMRAY 1820D SEM (Amray Inc., Bedford, MA).

Extraction, amplification, and sequencing of rDNA. Infected *T. cylindrica* collected from the Rhode River in January and December 2008 were incubated as described above for SEM observations. During incubation, nine host loricae containing sporogenic stages of *T. acutus* n. g., n. sp., but lacking host cells were selected for DNA extraction. Five specimens were preserved in iodine solution (final concentration of 0.04% [w/v] iodine; 0.06% [w/v] potassium iodide) and stored at 4 °C until DNA extraction, and four were frozen individually at − 20 °C in 40 μl sterile distilled water in a 1.5-ml Fisherbrand microcentrifuge tube (Thermo Fisher Scientific Inc., Waltham, MA) without fixation. Two *E. fraknoii* loricae containing *D. collini* were isolated and preserved in iodine solution.

Before DNA extraction, iodine-preserved specimens were rinsed through six drops of pico-pure distilled water and transferred individually to 40-μl sterile distilled water in a 1.5-ml Fisherbrand microcentrifuge tube. Frozen specimens were thawed, but not rinsed before DNA extraction. Each tube containing a single host lorica with parasite was sonicated using a probe tipped sonicator (Heat Systems Ultrasonic Inc., Model W-225R, Plain View, NY) set to a power level of 3 and a 30% duty cycle with three to five pulses over a 5-s internal. The resulting sonicate was used as template for polymerase chain reaction (PCR).

For *Scrippsiella trochoidea* (CCMP 2771), DNA was extracted from 50 ml of late log-phase culture grown at 20 °C in F/2 media (Guillard and Ryther 1962), with cool white fluorescent lamps providing irradiance at 100 μmol/m^2/s. The culture was harvested by centrifugation at 3,000 *g* for 10 min, the supernatant decanted, and the cell pellet stored at − 80 °C. Dinospores of *Amoebophrya* sp. from *Akashiwo sanguinea* and *Amoebophrya* sp. from *Gymnodinium instriatum* were harvested from infected host cultures following methods of Coats and Park (2002). Dinospore suspensions were centrifuged and frozen as above.

DNA was isolated using a CetylTrimethyl Ammonium Bromide (CTAB) detergent solution (Sigma, St. Louis, MO) following methods of Doyle and Doyle (1987). The CTAB buffer contained 2% (w/v) CTAB, 0.7 M NaCl, 100 μm Tris pH 8.0, and 10 μm EDTA. One milliliter of CTAB buffer was added to the cell pellet, mixed, and incubated at 65 °C for 10 min, cooled to room temperature, and 1 ml chloroform added. After mixing of the organic and aqueous phases and further incubation for 5 min at room temperature, the phases were separated by centrifugation at 10,000 *g* for 10 min. The aqueous phase was precipitated with 1 ml of 100% isopropanol, centrifuged as above for 10 min, washed with 70% ethanol, and resuspended in 100 μl of water. The genomic DNA was quantified using spectrophotometry and diluted to 50 ng/μl for PCR.

The rDNA region, about 3.5 kb of SSU, ITS1, 5.8S, ITS2, and LSU was amplified by PCR with three overlapping primer pairs: Euk A/B, Dino 1662F/25R1, or 25F1/LSUR2 (Handy et al. 2009). For the two *Amoebophrya* spp. a modified Dino 1662F primer was used (5′-CGGATTGAGTGWTCCGGTGAATAA-3′). Polymerase chain reactions were run in 20-μl reaction volumes containing template (100 ng in a 2-μl volume for cultures; 4–10 μl for sonicated single cells), 500 mg/ml BSA (Sigma A2053), 50 μm Tris HCl (pH 8.3), 3 μm $MgCl_2$, 10 μM dNTPs, 0.2 μM of each forward and reverse primers, and 0.12 U of Taq DNA polymerase (Promega Go-Taq, Madison, WI). The reactions were conducted in a Biometra T-gradient thermocycler (Biometra, Goettingen, Germany) using the following conditions: an initial denaturing step at 94 °C for 2 min, followed by 35 cycles of 94 °C for 15 s, 55 °C for 15 s, and 72 °C for 1.5 min, and a final extension at 72 °C for 5 min. Amplicons were visualized on 1% agarose gels stained with ethidium bromide, purified by polyethylene glycol precipitation (Morgan and Soltis 1995), washed with 70% ethanol, and resuspended in 10 μl pico-pure distilled water. Sequencing was done with 11 primers (EukA, SR3, SR4, SR5, SR8, SR9, EukB for the SSU; Dino1662 or the *Amoebophrya* variant as needed, 25F1, 25R1, LSUR2 for the ITS and LSU regions; Handy et al. 2009) using a Big-Dye Terminator v3.0 Cycle Sequencing kit (Applied Biosystems, Foster City, CA) and an ABI model 3730 sequencer (Applied Biosystems), according to the manufacturer's protocols. The amplicons were sequenced until at least double-stranded coverage was reached. Sequencher 4.8 (Genecodes, Ann Arbor, MI) was used to remove low-quality regions and assemble the individual sequence reads. The sequences were deposited in GenBank, with accession numbers listed in figures and supplemental material.

Alignments. To place the novel *T. acutus* n. g., n. sp., *D. collini*, and *S. trochoidea* sequences into context, an alignment of 88 SSU rDNA sequences (hereafter, SSU alignment) was compiled to encompass 86 dinoflagellates as in-group taxa with 63 identified to species, 18 to genus, and five to class, and two *Perkinsus* species as an outgroup. The alignment included sequences from all known genera of parasitic dinoflagellates for which data were available in GenBank (20 sequences from 12 genera). An additional 23 sequences were selected for inclusion in the alignment based on BLASTN searches using the novel sequences from this study as queries. The sequences were selected based on BLASTN identity ($\geq$ 95% to *T. acutus*; $\geq$ 98% to *D. collini* or *S. trochoidea*), where bitscores and query coverage were high ($\geq$ 2,875 and $\geq$ 96% to *T. acutus*; 3,074 and $\geq$ 97% to *D. collini* or *S. trochoidea*). The BLAST tree widget was used to screen for identical sequences, with redundant sequences eliminated. When different length redundant sequences were available, the longer sequence was selected. Sequences of another 39 dinoflagellates not identified in the queries above were included to broaden taxonomic coverage and provide intensive sampling of genera most closely related to *T. acutus* (i.e. 13 sequences representing *Pfiesteria*, *Pseudopfiesteria*, and *Luciella*) and *D. collini* (i.e. eight non-redundant sequences representing *Scrippsiella* and *Peridinium*). Finally, environmental clone sequences were excluded from the alignment. Sequences were aligned using CLUSTALX 1.83 (Thompson et al. 1997) and adjusted manually using MacClade 4.08 (Maddison and Maddison 2002). Highly variable regions of the alignment were removed using Gblocks (Castresana 2000) with default parameter settings, except that minimum length of a block was set to five bases and the gap parameter was set to half positions.

A longer rDNA sequence alignment, hereafter termed the SSU–LSU alignment, included the SSU, ITS1, 5.8S, ITS2, and LSU regions of *T. acutus*, *D. collini*, and *S. trochoidea*, the two strains of *Amoebophrya* as an outgroup, and 29 other taxa in the SSU alignment for which sufficient data were available in GenBank.

Phylogenetic analysis. Phylogenetic trees were inferred with maximum likelihood (ML), ML distances with minimum evolution, and Bayesian inference. Modeltest v.3.7 (Posada and Crandall 1998) was used to select the most appropriate model of substitution for the ML and ML-distance methods. The GTR+I+Γ (i.e. general time reversible with invariant sites and gamma rate correction) model was identified as the best-fit model for both the SSU and the SSU–LSU datasets.

Maximum likelihood analyses were performed using RAxML with the rapid bootstrapping option and 1,000 replicates (Stamatakis 2006). Trees were visualized and graphic versions exported using FigTree v1.2.2. ML-distance analyses were performed using PAUP* 4b10 (Swofford et al. 2002), with the parameters obtained from the best-fit model (GTR+I+Γ) of nucleotide substitution. Heuristic tree searches were started with a stepwise random addition of taxa with 10 replicates, followed by a tree-bisection-reconnection (TBR) branch-swapping algorithm. Maximum likelihood-distance bootstrapping was executed with 1,000 replicates starting from a neighbor joining tree and followed by TBR branch swapping.

Bayesian analysis used MrBayes 3.1.1 (Huelsenbeck and Ronquist 2001) running four simultaneous Monte Carlo Markov Chains for 2,000,000 generations and sampling every 100 generations, following a burn in of 100,000 generations.

Taxa and GenBank accession numbers used to infer phylogenetic trees are provided in supplemental material and are indicated in the figures.

RESULTS

Description of *Tintinnophagus acutus* Coats n. g., n. sp (Table 1–3; Fig. 2–27). All life-history stages of *T. acutus* lacked chloroplasts, as indicated by the absence of chlorophyll *a* autofluorescence under blue–violet excitation. Early in the infection cycle, *T. acutus* measured 13–18 × 14–20 μm in vivo (Table 1) and appeared as a hyaline orb typically attached to the host stalk (Fig. 2). These colorless cells lacked flagella, were connected to the host by a thin feeding tube, and contained an acentric, roughly spherical nucleus with a large central nucleolus (Fig. 2 inset). Growth of the parasite was accompanied by the formation of a conspicuous food vacuole (Fig. 3 inset) located in the upper half of the cell (i.e. toward the oral opening of the host lorica) and near the origin of the feeding tube. With continued feeding and growth, the cytoplasm of the parasite trophont became opaque due to the presence of numerous translucent granules, while the food vacuole became red to dark brown in color (Fig. 3–7). Numerous short rod-like chromosomes were evident in the nucleus of small to medium-size trophonts (Fig. 5), but were less conspicuous as the parasite matured (Fig. 6).

At the end of the growth phase, the mature parasite measured 36–48 × 72–108 μm (Table 1) before undergoing a series of sporogenic divisions to produce 18–46 dinospores (29.8 ± 3.7; $n = 8$). The first division was marked by migration of the translucent granules toward the equator of the cell, as the nucleus divided transversely (Fig. 7). The second fission was also transverse in most instances, producing four equal-sized sporocytes arranged sequentially within the host lorica (Fig. 8). The food vacuole did not divide and usually passed to the most anterior of the first four sporocytes. The third sporogenic division typically occurred perpendicular to the first and second fissions, with orientation of subsequent divisions difficult to assess (Fig. 9). The sporocyte receiving the residual food vacuole often divided more slowly than the others and sometimes failed to fully differentiate into dinospores. Sporocytes eventually appeared as a compacted mass in the posterior half of the host lorica (Fig. 10). Condensed chromosomes were clearly visible in the nuclei of sporocytes (Fig. 11), and some of the cells had two short flagella. The host often survived infection, remaining within the lorica even though its peduncle was usually ruptured during growth and sporogenesis of the parasite. On some occasions, however, the host abandoned its lorica before the parasite completed sporogenesis. In such specimens, the mass of sporocytes eventually disaggregated as the individual cells began to move in brief, short jumps. In several

Table **1.** Morphological attributes for *Tintinnophagus acutus* n. g., n. sp. trophonts in vivo.

	Range	Mean ± SE	Sample size
Trophonts			
Cell width	12.8–47.6	28.6 ± 1.76	31
Cell length	13.7–108.2	42.9 ± 4.42	31
Early infections[a]			
Cell width	12.8–18.4	15.0 ± 0.88	7
Cell length	13.7–19.8	17.4 ± 0.80	7
Mature parasites[b]			
Cell width	35.5–47.6	40.2 ± 2.62	4
Cell length	71.5–108.2	89.2 ± 7.53	4

Measurements are in μm, with mean given ± standard error (SE) to the mean.

[a]Trophonts that lacked food vacuoles and associated pigmentation.

[b]Specimens in first nuclear division, but lacking a distinct fission furrow.

Table **2.** Morphological attributes for living, preserved, and stained dinospores of *Tintinnophagus acutus* n. g., n. sp.

	Range	Mean ± SE	Sample size
Specimens in vivo			
Cell width	8.7–11.6	10.5 ± 0.42	7
Cell length	12.7–15.7	14.7 ± 0.39	7
Episome length	8.4–9.6	9.0 ± 0.18	7
Hyposome length	4.2–5.6	5.7 ± 0.29	7
Angle at cell apex	70.0–76.6	73.0 ± 0.80	7
Glutaraldehyde fixed specimens			
Cell width	7.6–12.4	9.9 ± 0.34	17
Cell length	11.2–17.4	13.6 ± 0.48	17
Episome length	6.3–9.7	7.5 ± 0.28	16
Hyposome length	4.4–8.2	6.3 ± 0.25	16
Angle at cell apex	63.9–71.7	69.1 ± 0.54	16
Length of trailing flagellum	22.0–30.3	25.1 ± 1.22	6
Protargol stained specimens			
Cell width	7.8–8.9	8.4 ± 0.11	11
Cell length	10.7–14.1	12.2 ± 0.28	11
Episome length	5.9–8.1	7.2 ± 0.20	11
Hyposome length	4.1–6.1	5.0 ± 0.16	11
Angle at cell apex	69.5–78	72.1 ± 0.77	10
Nuclear width	4.6–7.0	5.9 ± 0.26	11
Nuclear length	5.6–7.7	6.2 ± 0.18	11
Number of nucleoli	2–5	3.9 ± 0.34	11
Nucleolar width	0.5–1.9	1.1 ± 0.05	41
Nucleolar length	0.6–2.3	1.4 ± 0.07	41

Measurements are in μm, with mean given ± standard error (SE) to the mean.

Table **3.** Morphological attributes for protargol-stained trophonts of *Tintinnophagus acutus* n. g., n. sp.

	Range	Mean ± SE	Mode	Sample size
Cell length	6–85	—	—	252
Cell width	5–36	—	—	252
Nuclear length	5–25	—	—	252
Nuclear width	4–21	—	—	252
Nucleolar number	1–5	1.7 ± 0.1	1.0	252
Nucleolar diameter[a]	2–9	5.2 ± 0.1	4.0	178

Measurements are in μm, with mean given ± standard error (SE) to the mean.

[a]From specimens with only one nucleolus.

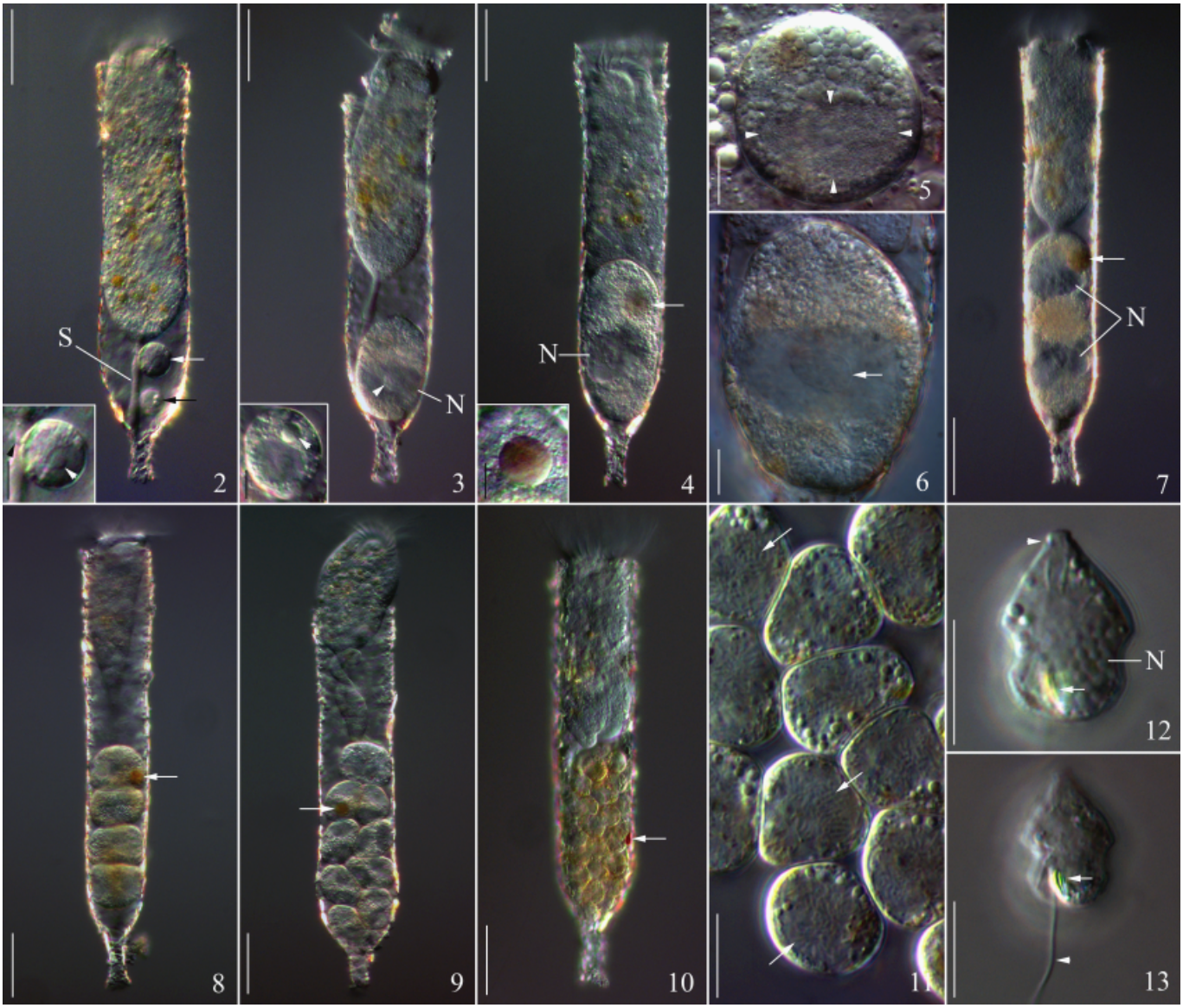

Fig. **2–13.** In vivo infection of *Tintinnopsis cylindrica* by *Tintinnophagus acutus* n. g., n. sp. Scale = 40 μm for Fig. 2–4 and 7–10. Scale = 10 μm for Fig. 5, 6, 11–13, and all insets. **2.** Two early stage infections (arrows) attached to the host stalk (S). Inset. Enlargement of the specimen indicated by white arrow. Note the feeding tube connecting the parasite to the host stalk (black arrowhead) and the acentrically positioned nucleolus (white arrowhead). **3**. Mid-stage infection with large ovoid nucleus (N) containing a single large nucleolus (arrowhead). Cytoplasm adjacent to the nucleus is opaque due to numerous small granules. Inset. Early infection with a small translucent food vacuole (arrowhead). **4**. Late infection with large nucleus (N) and red food vacuole (arrow). Inset. Enlargement of the red food vacuole. **5**. Mid-stage infection at high magnification showing short rod-like chromosomes within the ovoid nucleus (nuclear margins indicated by white arrowheads). **6**. High magnification of a late infection showing single large nucleolus and yellow to white translucent granules surrounding the ovoid nucleus. **7**. Early sporogenesis with cytoplasmic granules clustered equatorially, two nuclei (N), and a red food vacuole (arrow) located anteriad (i.e. toward the oral end of the host lorica). **8**. Four to eight cell stage of sporogenesis with food vacuole (arrow) in the anterior most daughter cell. **9**. Mid-sporogenesis with residual food vacuole (arrow) in subterminal daughter cell. **10**. Late sporogenesis with residual food vacuole (arrow) equatorial in the cluster of daughter cells. **11**. Late sporocytes with yellowish pigmentation, translucent granules, and short rod-like chromosomes (arrows). **12**. Dinospore showing chromosomes within the nucleus (N), crescent-shaped eyespot (arrow), and apical ''knob'' (arrowhead). **13**. Same specimen as Fig. 12 with eyespot (arrow) and training flagellum (arrowhead) in focus.

instances, the sporocytes moved out of the host lorica before fully differentiating into dinospores.

Mature dinospores were small, dinokont cells with a sharply pointed episome, rounded hyposome, clearly defined chromosomes, and a conspicuous yellow to orange, crescent or rod-shaped eyespot located near the origin of the flagella (Fig. 12, 13). Dinospores measured 13–16 × 9–12 μm in vivo and 11–17 × 8–12 μm after glutaraldehyde fixation (Table 2). The episome was slightly longer than the hyposome, appeared rigid, formed an apical angle of 70–80°, and had a noticeable anterior constriction that set the apex apart as a short cylinder (Fig. 12, 14). The sulcus was broad posteriorly, narrowed toward the girdle, and lacked a conspicuous anterior extension. The proximal and distal ends of the girdle were offset by about half the width of the girdle (Fig. 14). The trailing flagellum was 20–30 μm long. Dinospores readily attached to the body of host cells that had abandoned their lorica.

Protargol-stained dinospores measured 11–14 × 8–9 μm (Table 2) and had a large ovoid to reniform nucleus (5–7 μm maximum dimension) positioned posteriorly in the cell (Fig. 15). The nucleus contained two to five small nucleoli and was tightly packed with short, rod-like chromosomes (Fig. 15). Scanning electron microscopy revealed the presence of mastigonemes on the transverse flagellum, a thin, pointed peduncle at the base of the trailing flagellum, and a ''donut-shaped'' apical ''knob'' (Fig. 16,

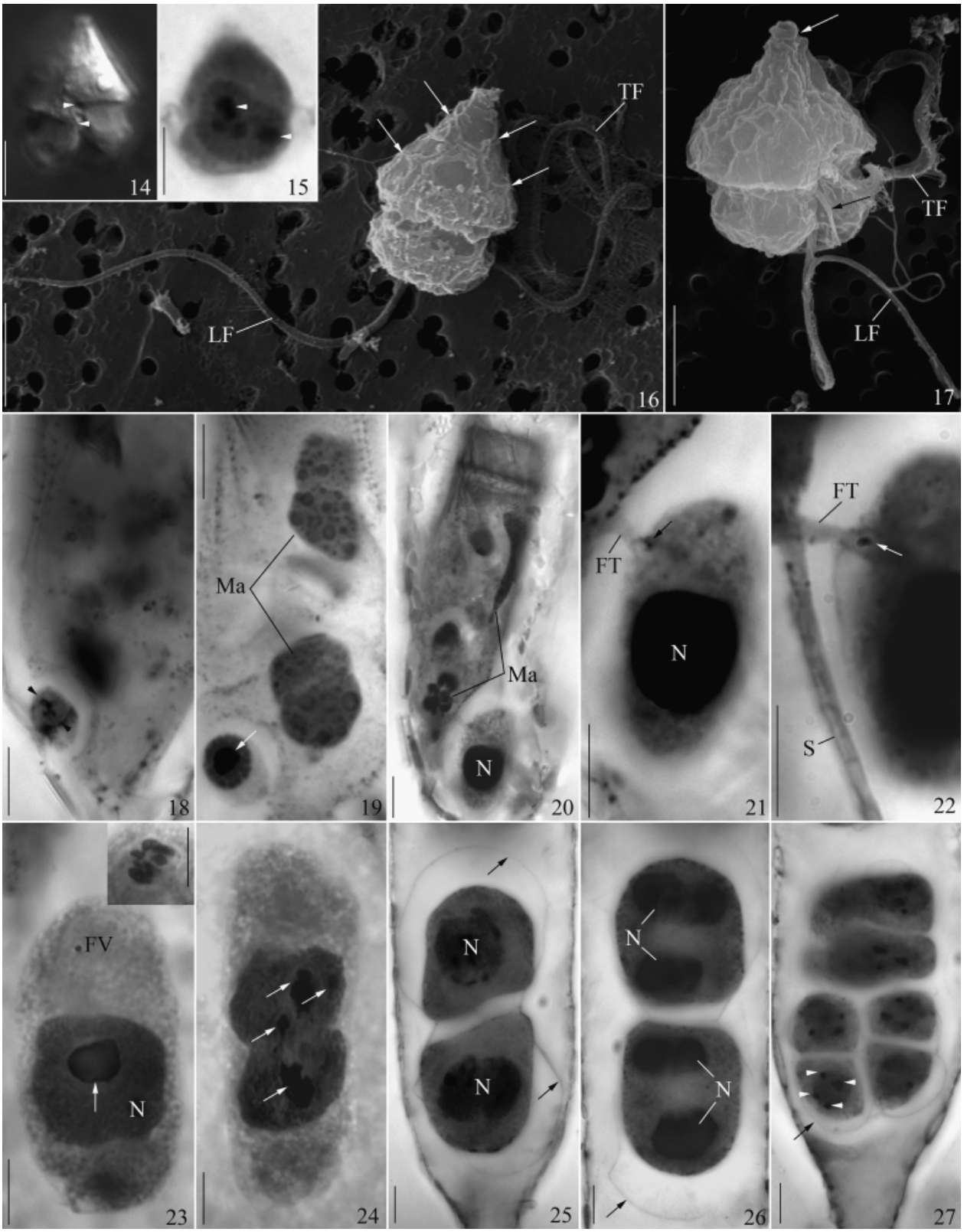

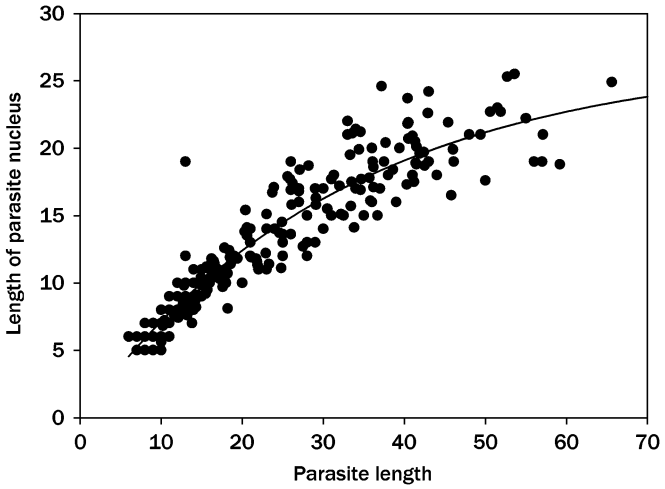

Fig. **28.** Nuclear size (microns) plotted against cell size (microns) for protargol-stained *Tintinnophagus acutus* n. g., n. sp. Data conform to a curvilinear regression (solid line) having an exponential rise to a maximum ($r^2 = 0.867$; $P < 0.01$; $n = 153$).

17). Attempts to visualize thecal plates of dinospores using calcoflour staining and SEM were unsuccessful. However, some specimens showed partially stripped membranes that appeared to delineate thecal sutures (Fig. 16).

Once attached to its host, *T. acutus* had a spherical to ovoid nucleus that increased in size with cell growth (Fig. 18–20, 23, 28). Young trophonts had conspicuous, densely staining chromosomes (Fig. 19). Nucleolar number ranged from 1 to 5, with mean number of nucleoli in 5–7 μm trophonts being about half that of dinospores (Table 3; Fig. 29). The number of nucleoli per cell decreased during early growth of the parasite, stabilizing at about 1.5 in trophonts > 10 μm in length. The multiple small nucleoli of early infections were usually clustered near the center of the nucleus (Fig. 18), while slightly larger trophonts (Fig. 19) generally had a single large nucleolus (Fig. 19, 23), suggesting coalescence of the multiple small nucleoli into a single nucleolus. The ''coalescenced'' nucleolus increased in size as the nucleus became larger (Fig. 30).

Early in the infection process, protargol-stained host cells had macronuclei typical in appearance to those of uninfected cells (i.e. ovoid with a lightly staining nucleoplasm, numerous dark granules, and in some instances a replication band; Fig. 19). By the middle of the infection cycle, however, host nuclei were highly elongated or broken into globular fragments (Fig. 20). The feeding tube was clearly visible in some specimens and had two argentophilic granules at its proximal end (Fig. 21). These granules, presumably basal bodies, did not have associated flagella. On rare occasions, a small food particle was present in the feeding tube. Food particles appeared to coalesce into a single large food vacuole that often contained densely staining material similar to that of fragmented host macronuclei (Fig. 23).

The nucleus of mature parasites was granular in appearance due to the presence of numerous small chromosomes and usually contained a single large nucleolus (Fig. 23). With the onset of sporogenesis, the nucleolus separated into numerous fragments that were distributed to daughter nuclei along with the chromosomes (Fig. 24–27). Each cell division occurred within a thin, seemingly rigid outer membrane or cyst wall (Fig. 25–27).

***Tintinnophagus acutus* n. g., n. sp. development time and effect on host cells.** When incubated at 6–8 °C in filtered estuarine water, early infections by trophonts 5–10 μm in diameter required approximately 4 d to mature and another 2 d to complete sporogenesis (Table 4). Ignoring the time required for dinospores to encounter new host cells, generation time of *T. acutus* was about 6 d.

Host cells supporting mature *T. acutus* were visibly smaller than uninfected organisms, indicating that utilization of host biomass by the parasite exceeded host growth rate. In protargol-stained material, parasite biovolume was roughly 3X that of the host and represented $71 \pm 4.4\%$ of the total biomass of host+parasite. In addition to being smaller in size and having disrupted macronuclei, infected hosts appeared to lose the ability to reproduce, as indicated by the proportion of cells undergoing stomatogenesis (Fig. 31, 32). While $\sim 50\%$ of uninfected *T. cylindrica* had developing oral structures for their posterior daughter cell, only 18% of infected host cells showed signs of stomatogenesis. Furthermore, uninfected hosts were equally partitioned as early and late stages of stomatogenesis, while very few infected hosts ($< 1\%$) had progressed to late stomatogenesis.

***Duboscquodinium collini* from *Eutintinnus fraknoii*.** *Dubosquodinium collini* measured $55 \pm 2.9 \times 29 \pm 0.8$ μm, with individuals being tightly lodged in the lorica of their host (Fig. 33). None of the loricae was occupied by living host cells, but some showed cellular debris apparently derived from recently dead host organisms. In those instances, the parasite was located above the remains of the host (i.e. toward the oral opening of the lorica). *Dubosquodinium collini* lacked obvious pigmentation and chlorophyll *a* autofluorescence, but possessed a large food vacuole, a small spherical nucleus with condensed chromosomes, and a thin outer membrane or cyst wall that had an acute peak directed

Fig. **14–27.** Dinospore morphology and cytology of *Tintinnophagus acutus* n. g., n. sp., during infection of *Tintinnopsis cylindrica*. Scale = 5 μm for Fig. 14–17 and 10 μm for Fig. 18–27. **14**. Dinospore in vivo demonstrating offset of the girdle. Arrowheads mark the anterior margin of the girdle at its proximal and distal ends. **15**. Protargol-stained dinospore illustrating the posteriorly positioned ovoid to reniform nucleus, multiple nucleoli, and condensed chromosomes giving the nucleoplasm a marbled appearance. **16**. Scanning electron microscopy (SEM) of the dorsal surface of a dinospore with partially ''stripped'' cell membranes, longitudinal flagellum (LF), and transverse flagellum (TF). Arrows indicate membranous material adhering to potential margins of thecal plates. **17**. SEM of a dinospore in ventral perspective showing the peduncle, apical ''knob,'' and origin of the transverse (TF) and longitudinal (LF) flagella. 18–27. Protargol silver-impregnated specimens. **18**. A recently attached trophont having multiple, coalescing nucleoli within the nucleus. Arrowheads indicate the perimeter of the parasite nucleus. **19**. Slightly later stage of infection with a single nucleolus (arrow) and short, densely packed chromosomes. Host macronuclei (Ma) have an appearance typical of uninfected cells. **20**. Mid-stage infection with large ovoid nucleus (N). One host macronucleus (Ma) is atypically elongate, while the other is broken into multiple densely staining fragments. **21**. Higher magnification of the same specimen in Fig. 20 showing a pair of argentophilic granules (arrow) at the proximal end of the feeding tube (FT). **22**. Another mid-stage infection with a densely staining body inside a food vacuole (arrow) located in the feeding tube (FT); host stalk (S). **23**. Late infection with food vacuole (FV) and large nucleus (N) containing a densely staining nucleolus and lightly stained chromosomes. Inset. Several dark bodies contained in the food vacuole (FV) of another late infection. **24**. First sporogenic division showing multiple nucleoli (arrows) and chromosomes aligned along the axis of nuclear fission. **25**. Two-cell stage of sporogenesis with daughter nuclei (N) entering the next fission. Note outer membrane (arrows) surrounding each cell. **26**. Two-cell stage following second nuclear division. Arrow indicates outer membrane. **27**. Eight to 16-cell stage of sporogenesis showing multiple nucleoli (arrow heads) in each nucleus and outer membrane surrounding each daughter cell.

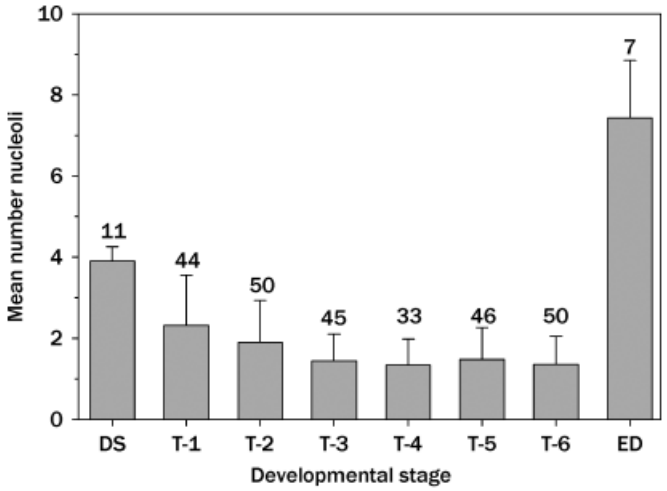

Fig. **29.** Mean nucleolar number for dinospores (DS), trophonts partitioned by nuclear length (T-1 = 5–7 μm; T-2 = 8–10 μm; T-3 = 11–13 μm; T-4 = 14–16 μm; T-5 = 17–19 μm; T-6 ≥ 19 μm), and specimens undergoing the first sporogenic division (ED) of *Tintinnophagus acutus* n. g., n. sp. Standard error of the mean and sample size is indicated for each category. Data are for protargol-stained specimens.

toward the oral opening of the host lorica (Fig. 33, 34). After fixation, the outer membrane was distended away from the cell forming a smooth covering with little or no indication of the peak evident in living specimens (Fig. 35). Protargol-stained specimens showed food vacuoles in various states of digestion, nuclei with condensed chromosomes, and karyokinesis typical of dinoflagellates (Fig. 36, 37).

rDNA sequences. The rDNA region of *T. acutus* n. g., n. sp. was 3,619 nucleotides in length and was successfully amplified from nine individuals in late sporogenesis. All specimens were collected from the Rhode River, MD, USA with one obtained in January 2008 and eight in December 2008. Sequences for specimens isolated in December were fully resolved and were identical. The sequence of the single specimen from January had four

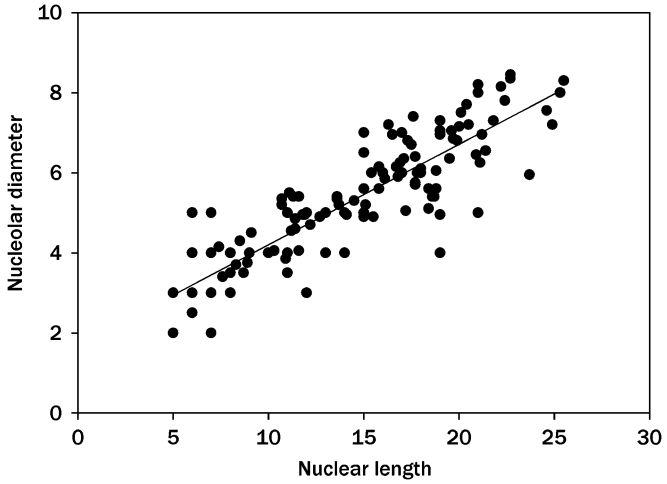

Fig. **30.** Nucleolar diameter (μm) relative to nuclear size (μm) for protargol-stained trophonts of *Tintinnophagus acutus* n. g., n. sp. Data have a significant positive correlation ($r^2 = 0.873$; $P < 0.01$; $n = 137$). Linear regression (solid line) added for visualization of the relationship.

Table **4.** Generation time of *Tintinnophagus acutus* n. g., n. sp. partitioned as time required for trophont growth and sporogenesis.

Growth stage	Mean ± SE	Range	Sample size
	Time (h); [d]	Time (h)	(*n*)
From 5 to 10 μm trophont to first division	90 ± 6 [3.8 ± 0.25]	52–125	14
First division to release of dinospores	52 ± 5 [2.2 ± 0.21]	31–72	9
Generation time[a]	146 ± 7 [6.1 ± 0.29]	102–172	9

[a]Calculated as duration of trophont growth plus duration of sporogenesis.

ambiguous base positions in the ITS regions, but was otherwise identical to the other eight sequences. BLASTN searches of GenBank provided a 96% maximum match of the *T. acutus* SSU rDNA sequence to representatives of other dinoflagellate genera, including *Paulsenella* (AJ968729), *Pentapharsodinium* (AF022201; AF274270), *Peridinium* (AY443018), *Prorocentrum* (EU780638; Y16232), *Scrippsiella* (AM494499; AB183677; AF274276), and *Stoeckeria* (FN557541).

Two *D. collini* individually isolated from a single sample collected from the Bay of Villefranche-sur-Mer, France in September 2009 yielded rDNA sequences of 3,009 and 3,620 nucleotides, with discrepancy in length due to incomplete sequencing of the LSU rDNA. The sequences differed by one base position in the SSU and five in the ITS through the LSU regions (0.06% difference in the SSU rDNA; 0.2% overall). A BLASTN query matched the SSU rDNA of *D. collini* to *Scrippsiella* spp. (AB183677, AF274277, AJ415515, AM494499, AY743960) with 99% identity. A BLASTN query using the SSU sequence of *Scrippsiella trochoidea* (CCMP 2771; total sequence length = 3,530 nucleotides) gave identical results to those obtained for queries using *D. collini*.

Comparison of the SSU rDNA sequences showed marked difference between *T. acutus* and *D. collini* (63 bases; 3.5%). The SSU rDNA of *D. collini* and *S. trochoidea*, however, differed by only four bases (0.2%). Sequence divergence was greater when compared across the entire rDNA region, with *T. acutus* and *D. collini* differing by 331 bases (9.1%), while *D. collini* and *S. trochoidea* differed by 84 bases (2.4%).

Phylogenetic analyses. Total length of the SSU alignment for 86 in-group taxa (i.e. seven syndinians and 79 dinophyceans) and two outgroup taxa (Perkinsozoa) was 1,807 bases, with sequence length ranging from 1,206 to 1,754 bases. Trimming the alignment using Gblocks left 1,706 positions for phylogenetic analyses.

The ML tree inferred from the SSU alignment had a ln value of −17486.960781 and is presented with ML bootstrap values, Bayesian posterior probability, and ML-distance bootstrap values (Fig. 38). The three analyses produced trees of comparable topology, showing a moderately supported split (ML and ML-distance bootstrap values >70%; posterior probability ≥ 0.90) between the Dinophyceae and Syndiniophyceae, with *T. acutus* n. g., n. sp. and *D. collini* nested among thecate dinoflagellates deep within the Dinophyceae. Clades representing the Suessiales, including the fish parasite *Piscinoodinium* sp., *Prorocentrum*, *Heterocapsa*, and a prominent ''*Pfiesteria* group'' containing *Luciella masanensis*, *Cryptoperidiniopsis* species, *Pseudopfiesteria shumwayae*, and *Pfiesteria piscicida* were well supported (ML and ML-distance bootstrap values >85%; posterior probability ≥ 0.95) and consistent across the phylogenies. A ''*Scrippsiella* group,'' including *Peridinium polonicum*, *D. collini* from *E. fraknoii*, and all but one of the *Scrippsiella* species (i.e. *S. hangoei*) was well supported by Bayesian and ML-distance analyses, but poorly supported by ML bootstrapping (<65%). Small

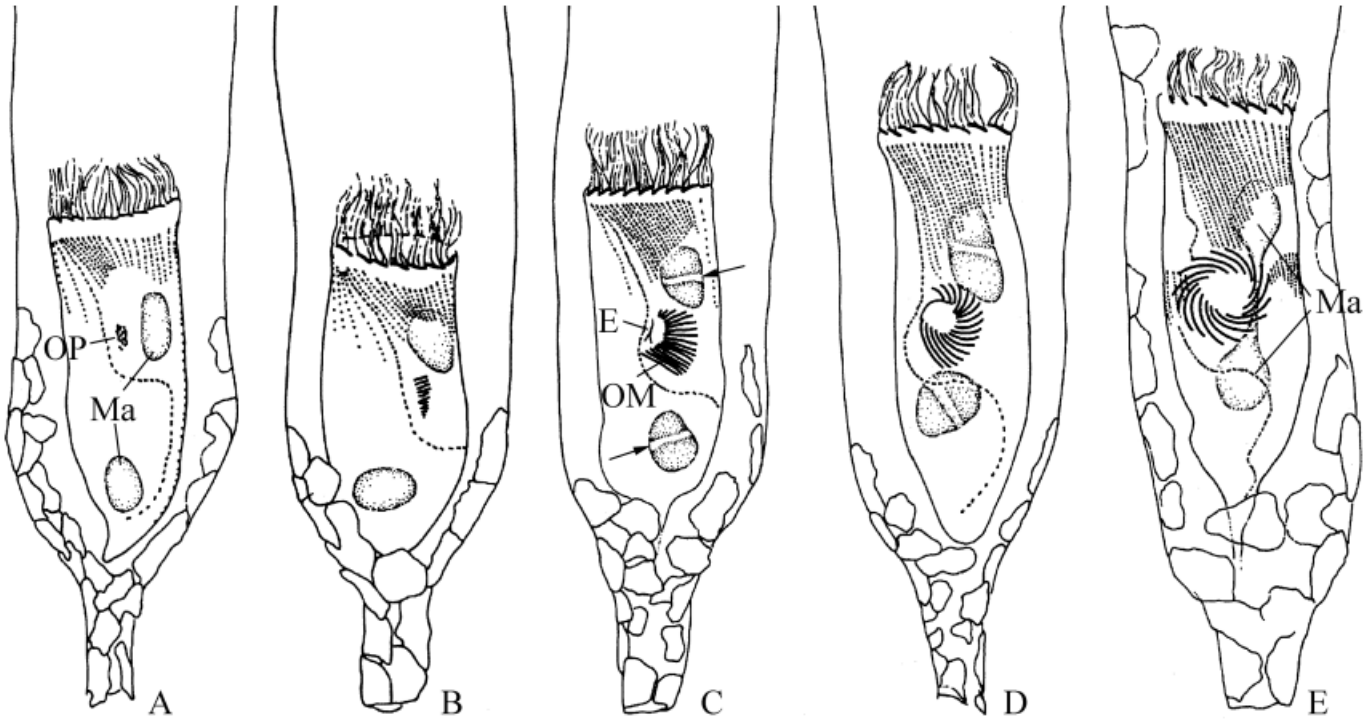

Fig. **31.** Semi-schematic representation of five sequential stages (A–E) in stomatogenesis of *Tintinnopsis cylindrica*, as revealed by protargol staining. For purposes of examining the effect of parasitism by *Tintinnophagus acutus* n. g., n. sp. on host reproduction, stages A–C were considered early stomatogenesis and stages D and E late stomatogenesis. Endoral membrane (E); macronucleus (Ma); oral membranelles (OM); oral primordium (OP); arrows indicate macronuclear replication bands. Illustration made using a Zeiss drawing tube.

subunit rDNA sequences clustered in the *Scrippsiella* group differed by a maximum of 1.6%, with the two sequences for *D. collini* differing from that of *S. sweeneyae*, type species for the genus, by only 0.3–0.4%. The genera *Haploozoon* and *Chytridinium* each formed a monophyletic lineage of parasites; however, their placement within the Dinophyceae was not well resolved. *Blastodinium* species from copepods consistently failed to group together and were polyphyletic. *Paulsenella vonstoschii*, a parasite of diatoms, branched adjacent to the *Pfiesteria* group with moderate support (i.e. bootstrap values of 65–80%, or posterior probabilities of 0.90–0.95). The positions of *Amyloodinium ocellatum*, a parasite of fish, and *T. acutus* from *T. cylindrica* were not well resolved, but each consistently branched outside the *Pfiesteria* group.

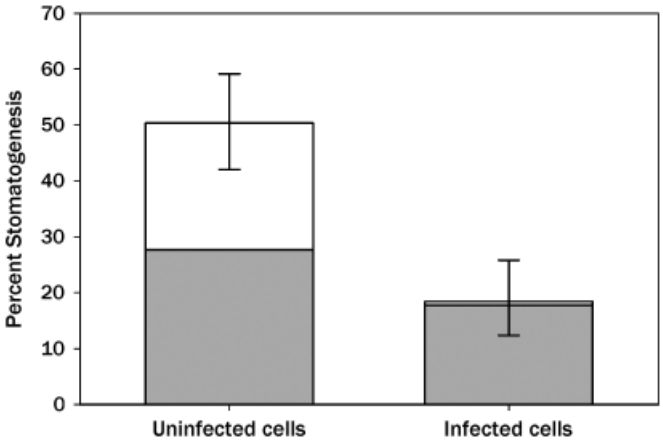

Fig. **32.** Proportion of *Tintinnopsis cylindrica* undergoing stomatogenesis when uninfected and infected by *Tintinnophagus acutus* n. g., n. sp. Gray and white portion of bars indicate early and late stomatogenesis, respectively (see Fig. 31). Error bars are 95% confidence limits; $n = 141$ for each host categories.

The SSU–LSU alignment of 29 in-group taxa and two *Amoebophrya* spp. as outgroup taxa was 4,188 nucleotides long, with individual sequence length ranging from 3,046 to 6,332 bases. After trimming with Gblocks, 2,853 positions remained for use in phylogenetic analyses. The selected positions represented 99% of the SSU rDNA, 16% of ITS1, 99% of the 5.8S, 11% of ITS2, and 58% of the LSU rDNA in the aligned dataset. The ML tree inferred from the SSU–LSU alignment had a ln value of − 16599.185661 (Fig. 39). The SSU–LSU trees were similar to the SSU trees in topology and were largely congruent across methods; however, disagreements were found using the ML-distance analysis (cf., Fig. 38, 39). The ''*Pfiesteria* group'' was a strongly supported clade in all three analyses with bootstrap values of 100% and posterior probability of 1.00 (Fig. 39). *Stoeckeria* sp. and the dinophycean ''Shepherd's crook'' formed a well-supported sister lineage to the ''*Pfiesteria* group,'' to which *T. acutus* and *D. collini* were consistently basal. *Dubosquodinium collini* and *S. trochoidea* grouped together with strong support in all three analyses (Fig. 39). Placement of *T. acutus* was less well resolved, as it fell between the *Stoeckeria*-''Shepherd's crook'' clade and the *Scrippsiella–Duboscquodinium* clade in ML and Bayesian analyses, but clustered with *S. trochoidea* and *D. collini* by the ML-distance method.

DISCUSSION

Comparison of *Tintinnophagus acutus* n. g., n. sp. with other dinoflagellate parasites of tintinnids. Haeckel (1873) noted the presence of 10–20 small, spherical cells in the cytoplasm of two

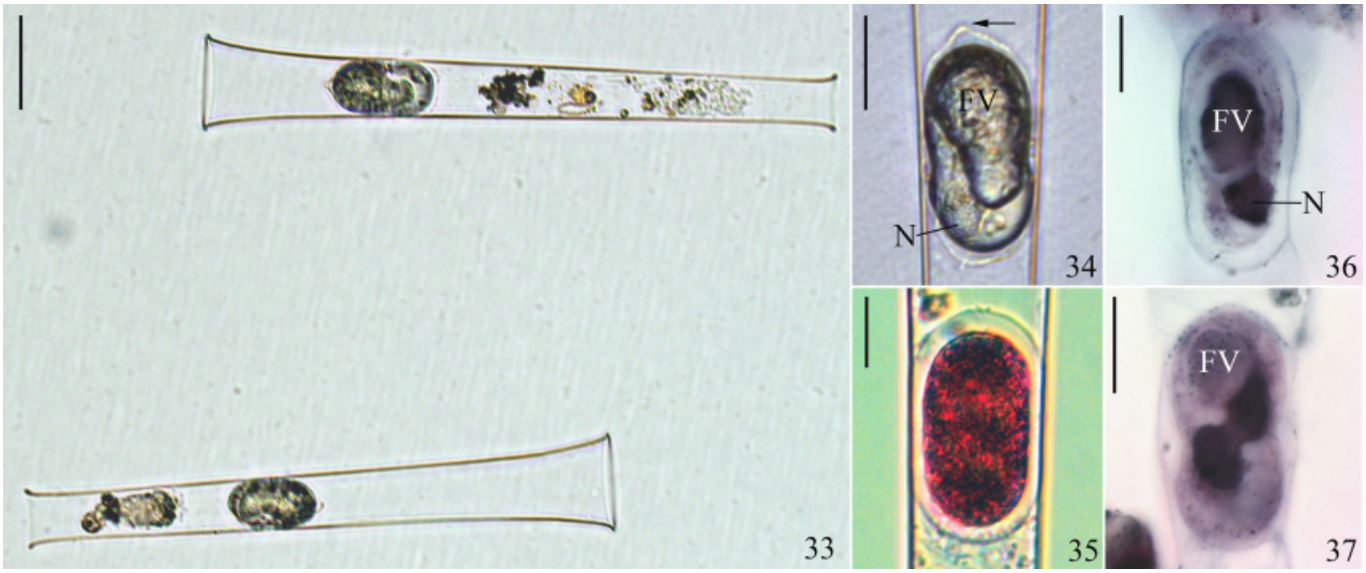

Fig. **33–37.** *Duboscquodinium collini* from *Eutintinnus fraknoii*. Scale = 20 μm, except 100 μm for Fig. 33. **33**. In vivo specimen in each of two host loricae. Debris in the posterior portion of the loricae is the remains of dead host cells. **34**. High magnification of the upper specimen in Fig. 33 showing a peak in outer membrane (arrow) directed toward the oral opening of the host lorica, nucleus (N) with condensed chromosomes, and large food vacuole (FV). **35**. Bouin's preserved specimen with more evenly spaced outer membrane lacking a distinct peak. **36**. Protargol-stained specimen with dinokaryotic nucleus (N) and food vacuole (FV). **37**. Specimen undergoing nuclear division and having reduced food vacuole (FV) contents; protargol stain.

tintinnid species, *Cyttarocylis cassis* (reported as *Dictyocysta cassis*) and *T. campanula* (reported as *Codonella campanella*), interpreting them to be ciliate reproductive propagules or spores. When removed from the ciliate, the ''spores'' lacked cilia or flagella and contained a spherical nucleus. In one *T. campanula*, Haeckel (1873) also reported larger (30 × 20 μm), uniformly ciliated cells that he interpreted to be ciliate embryos. Haeckel's spherical spores are now considered to be the first report of dinoflagellate parasitism in ciliates, being placed by Chatton (1920) in the genus *Duboscquella*, while the nature of the enigmatic ciliated ''embryos'' remains uncertain.

Several years later, Laackmann (1906, 1908) mistook parasitism of *T. campanula* and *Cyttarocylis helix* (basionym: *Tintinnus helix* Claparède & Lachmann, 1858; used hereafter) as sexual reproduction. His 1906 article provided an account, but no illustrations, of parasites, called sporocysts by Laackmann, which pinched off the posterior end of *T. campanula* and divided to produce either microspores or macrospores. Microspores and macrospores formed in separate host loricae and were, respectively, characterized as ∼ 5 μm spherical cells that numbered well over 100 per tintinnid and much larger gymnodinoid cells (17–20 μm long by 10–12 μm wide) that numbered 12–24. Arrangement and number of flagella were not determined, but spores were reported to move rapidly in a sinusoidal fashion while spinning around their longitudinal axis. Laackmann (1908) expanded his observations for *T. campanula*, noting that many specimens contained a darkly staining mass positioned posteriorly in the cell, but were otherwise normal in appearance. He interpreted these bodies as developing ''sporocysts'' (i.e. parasites) and provided an illustration (his Fig. 33) that conforms nicely in position, shape, and nuclear morphology to parasites now placed in the genus *Duboscquella* (Cachon 1964; Coats 1988; Coats et al. 1994). Laackmann (1908) also described parasite development in *T. helix*, including several illustrations, but never mentioning ''sporocysts'' in the cytoplasm of the host. Rather, host loricae contained a large cytoplasmic mass, presumably the tintinnid zooid, to which was attached a small ''sporocyst.'' In vivo, these small ''sporocytes'' gradually increased in size, while the cytoplasmic mass of the host cell diminished. Large ''sporocysts'' in *T. helix* eventually divided to produce gymnodinoid macrospores (his Fig. 21) that were similar in appearance and behavior to those observed in *T. campanula* (Laackmann 1906), but no microspores were reported. The gradual growth of parasites attached to the outside of *T. helix* and the lack of microspore formation, strongly suggest that Laackmann was dealing with two different dinoflagellates, an intracellular parasite in *T. campanula*, resembling a species of *Duboscquella*, and an extracellular parasite in *T. helix*, perhaps related to *T. acutus* n. g., n. sp.

Lohmann (1908) described colorless, parasitic gymnodinoid macrospores that emerged from the lorica of *Tintinnopsis nucula*

Fig. **38.** Maximum likelihood (ML) phylogenetic tree based on a small subunit (SSU) ribosomal DNA (rDNA) alignment of 86 dinoflagellate sequences, with two *Perkinsus* species as the outgroup. The alignment of 1,706 base positions (ln = − 17486.960781) included novel sequences for *Tintinnophagus acutus* n. g., n. sp., *Duboscquodinium collini*, and *Scrippsiella trochoidea* in bold. Representatives from all parasitic dinoflagellate genera with SSU rDNA sequences available in GenBank were included, as well as SSU rDNA sequences from GenBank with high identity to the novel *T. acutus*, *D. collini*, or *S. trochoidea* sequences. Representatives of other major dinoflagellate groups were also included. The alignment was analyzed using ML, ML-distance using minimum evolution, and Bayesian methods. In all cases, the optimal model was the GTR+I+Γ model. Bootstrap support values over 65% are indicated over nodes as ML/Bayesian posterior probability/ML distance. Branches with 100% support by bootstrapping and a *P*-value of 1.00 are indicated with a filled circle. The ''−'' symbol indicates absence of the branch in the optimal Bayesian or distance tree. The ''+'' symbol indicates presence of the branch on the optimal tree, but with bootstrap values below 65%, or Bayesian *P*-values were below 0.90. GenBank accession numbers are shown in parentheses. Branch lengths are shown in substitutions per site. Host species not indicated in the figure are: [a]*Axiothella rubrocinta*; [b]*Praxillella pacifica*; [c]*Akashiwo sanguinea*; [d]*Favella ehrenbergii*.

(now considered a species of *Stenosemella*, possibly *S. nivalis*, Agatha, pers. commun.). The spores were unquestionably dinoflagellates, numbered ~10 per tintinnid, were 18 μm long, and had a distinct girdle and sulcus with associated transverse and longitudinal flagella. Lohmann (1908) clearly illustrated macrospores of the parasite (his Fig. 6) and, in his figure legend, provided for them the new species name *Gymnodinium tintinnicola*. He believed *G. tintinnicola* to be an intracellular parasite,

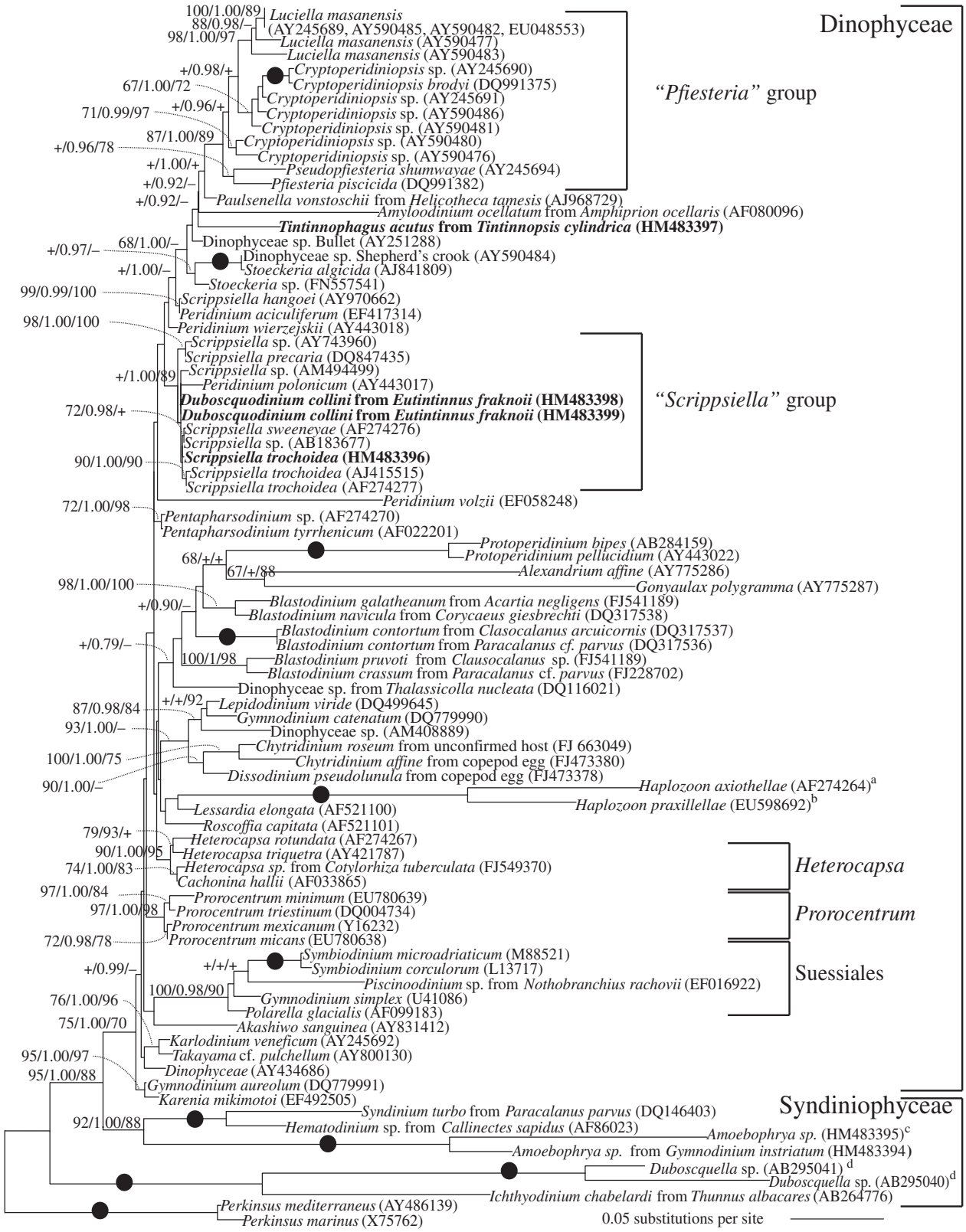

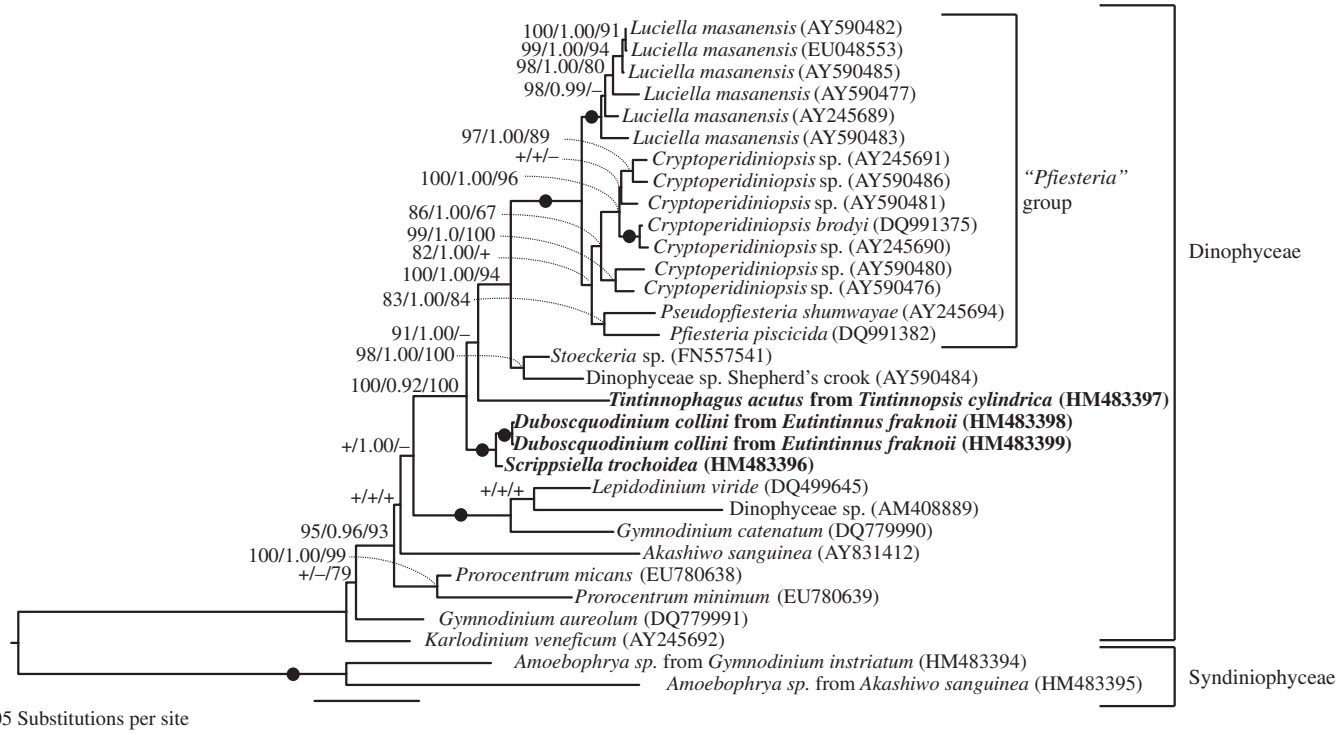

Fig. **39.** Maximum likelihood (ML) phylogenetic tree based on a small subunit to large subunit (SSU–LSU) ribosomal DNA alignment of 29 dinophycean sequences and two *Amoebophrya* species as the outgroup. The alignment of 2,853 base positions (ln = − 16599.185661) included novel sequences for *Tintinnophagus acutus* n. g., n. sp., *Duboscquodinium collini*, and *Scrippsiella trochoidea* in bold. Representatives from all parasitic dinoflagellate genera with contiguous SSU–LSU sequences available in GenBank were included, as well as SSU–LSU sequences from GenBank with $\geq$ 98% identity to novel *T. acutus*, *D. collini*, or *S. trochoidea* sequences. Representatives of other major dinoflagellate groups were also included. The alignment was analyzed using ML, ML-distance with the minimum evolution optimality criterion, and Bayesian methods. In all cases, the optimal model was the GTR+I+Γ model. Bootstrap support values from 100 replicates over 65% are indicated over nodes as ML/Bayesian posterior probability/ML-distance. Branches with 100% support by bootstrapping and a *P*-value of 1.00 are indicated with a filled circle. The ''−'' symbol indicates absence of the branch in the optimal Bayesian or distance tree. The ''+'' symbol indicates presence of the branch on the optimal tree, but with bootstrap values below 65%, or Bayesian *P*-values were below 0.90. GenBank accession numbers are shown in parentheses. Branch lengths are shown in substitutions per site.

although he did not report seeing the parasite in the cytoplasm of the host cell. Rather, his conclusion appears to be based on the account of ''sporocyst'' development provided by Laackmann (1908). In light of the discussion above, Lohmann's *G. tintinnicola* could be either an intracellular or an extracellular parasite.

Entz (1909) mentioned gymnodinoid spores produced by a parasite of *Favella ehrenbergii* (reported as *Cyttarocylis ehrenbergii*), but did not provide illustrations. A year later, Duboscq and Collin (1910) described what they interpreted as sexual reproduction in a dinoflagellate infecting *F. ehrenbergii*. While their account of the sexual cycle is likely erroneous (see Cachon 1964), their description and illustrations subsequently published in Chatton (1920), provided important details on the morphology of the parasite trophont and dinospores. The parasite trophont was clearly intracellular and closely resembled the intracellular ''sporocyte'' described in *T. campanula* by Laackmann (1908). Some specimens contained numerous intracellular sporocysts, similar to the report of Haeckel (1873), leading Duboscq and Collin (1910) to conclude that sporogenesis began inside the host and culminated in the extracellular release of dinospores. Because cell division of the parasite inside the host cytoplasm was not observed, it is probable that the numerous intracellular sporocysts seen by Duboscq and Collin (1910) in a single host actually represented multiple infections (see Coats et al. 1994). Unlike the gymnodinoid macrospores observed by Laackmann (1908) and Lohmann (1908), the parasite studied by Duboscq and Collin (1910) produced *Oxyrrhis*-like macrospores that had a pointed anterior portion, a rounded posterior end, and a pair of laterally placed flagella, one extending anteriad and one wrapping loosely around the cell.

Chatton (1920) created the genus *Duboscquella* to include parasites of *T. campanula* (Laackmann 1906), *Stenosemella* cf. *nivalis* (Lohmann 1908), and *F. ehrenbergii* (Duboscq and Collin 1910; Entz 1909). He also included Haeckel's ''ciliate embryos'' from *T. campanula*, mistakenly referring to the host as *Codonella galea*, but, as mentioned above, the status of those ''embryos'' is very uncertain. Chatton (1920) viewed infections of the various hosts as representing a single species of intracellular parasite and included all under the type species *Duboscquella tintinnicola* (Lohmann 1908) Chatton 1920. In making that decision, Chatton (1920) accepted the report of Duboscq and Collin (1910) as a redescription of *G. tintinnicola*, even though dinospore morphology was not consistent with that reported by Lohmann (1908). Seven additional species of *Duboscquella* have been subsequently described (Cachon 1964; Chatton 1952; Coats 1988), none of which produces dinospores having a clearly defined girdle and sulcus. Macrospores of *Duboscquella* species described in these more recent manuscripts have a rounded episome, cylindrical to conical hyposome, a trailing flagellum, and a transverse flagellum loosely wrapped around the cell. In many respects, they resemble an inverted form of the spores described by Duboscq and Collin (1910). The resemblance was sufficiently striking for

Cachon (1964) to suggest that Duboscq and Collin (1910) were mistaken about the polarity of their specimens.

Since Lohmann's (1908) account of *G. tintinnicola*, the only dinoflagellate parasites of tintinnids reported to have gymnodinoid spores belong to the genus *Tintinnophagus* (this manuscript) and *Duboscquodinium* (Grassé 1952 in Chatton 1952), the latter said to produce gymnospores, but no illustrations of the spore were provided. The descriptions provided by Grassé (1952 in Chatton 1952) for *D. collini*, the type species infecting *E. fraknoii*, and *D. kofoidi*, a parasite of *T. campanula*, are the only accounts of these parasites in the published literature. Cachon (1964), who worked extensively on parasites of protists in the Mediterranean Sea, did not encounter tintinnids infected by *Duboscquodinium*. Our specimens, obtained from a single, fortuitous sample taken from the Bay of Villefranche-sur-Mer, did not permit examination of the parasite's complete life cycle, but were sufficient to identify the organism as *D. collini* based on tomont morphology and host species. Aside from a distinctive peak in the outer membrane or cyst wall at one end of the parasite, our specimens conformed in all respects to the tomont of *D. collini*. Importantly, the peak was not present in all specimens, nor did it persist following fixation, suggesting that it is a transient feature, which could have been easily overlooked by Grassé (1952 in Chatton 1952).

Grassé (1952 in Chatton 1952) believed *D. collini* and *D. kofoidi* to be intracellular parasites, but did not report seeing infected host cells, as his observations were based on pre-sporogenic and sporogenic stages of the parasite in loricae devoid of host organisms. Our observations were likewise hampered by the absence of living hosts in loricae containing *D. collini*. Thus, we cannot comment on the nature of the parasitic relationship of *D. collini* with its host, or compare life styles (i.e. intra- vs. extracellular parasitism) of *Tintinnophagus* and *Duboscquodinium*. *Tintinnophagus acutus* resembles *D. collini* by its dinokaryotic nucleus with condensed chromosomes, conspicuous food vacuole in the trophont, and palintomic sporogenesis leading to gymnodinoid dinospores. However, *T. acutus* differs from *D. collini* by host species, the absence of an outer membrane or cyst wall surrounding pre-sporogenic stages, failure of the first sporogenic division to differentiate a trophocyte (i.e. non-dividing daughter cell that presumably continues to feed) and a gonocyte (i.e. daughter cell that continues to divide; = gametocyte of Grassé), and rDNA sequence (see below for further molecular comparison). Late in the sporogenesis of some specimens, however, *T. acutus* did produce a sporocyte that failed to divide further and eventually degenerated, as Grassé (1952 in Chatton 1952) reported for the trophocyte of *D. collini*. *Tintinnophagus acutus* differs from *D. kofoidi* by the absence of a ''rosace'' stage during sporogenesis and by host species. Were it not for this ''rosace'' stage, Grassé's description of *D. kofoidi* would correspond nicely with Laackmann's (1906, 1908) account of macrospore formation in *T. campanula*.

The striking difference in spore morphology between Lohmann's *G. tintinnicola* from *S.* cf. *nivalis* and the account provided by Duboscq and Collin (1910) for parasitism of *F. ehrenbergii* raises the possibility that the two studies may have been dealing with different parasitic organisms. Indeed, based on macrospore morphology, Lohmann's *G. tintinnicola* from *S.* cf. *nivalis* would seem more closely aligned with *Duboscquodinium* and *Tintinnophagus* than with other species currently included in the genus *Duboscquella*. Should future investigation of parasitism in *S.* cf. *nivalis* support that conclusion, then major restructuring of the genus *Duboscquella* would be indicated. In recognizing the possibility that *T. acutus* may be related to *D. tintinnicola* of Lohmann (1908), it is necessary to emphasize that the two organisms show important differences. While their dinospores are similar in size, those of *T. acutus* have a sharply pointed episome and a conspicuous eyespot at the base of the flagella. By contrast, the macrospores described by Lohmann (1908) had a smooth, rounded episome and lacked an eyespot.

Prior reports of parasitism in *Tintinnopsis cylindrica*. Parasites of *T. cylindrica* (= *kofoidi*) have been reported on three prior occasions, once without providing a taxonomic identification (Hada 1932) and twice as *Duboscquella* sp. (Agatha and Riedel-Lorjé 2006; Akselman and Santinelli 1989). Hada (1932) appears to have seen an intracellular parasite, with his illustrations being more or less consistent with a species of *Duboscquella*. Akselman and Santinelli (1989) provided a single illustration of parasite sporogenesis and insufficient description of the parasite to determine if they were working with a species of *Duboscquella*, *T. acutus*, or some other organism. The specimens of Agatha and Riedel-Lorjé (2006), however, were certainly parasitized by *T. acutus*, as their illustrations clearly show growth and sporogenesis of the extracellular parasite. They also report changes in the host macronucleus as the parasite ''sucks out the tintinnid cell.''

Phylogenetic placement of *Tintinnophagus acutus* n. g., n. sp. and *Duboscquodinium collini*. Historically, most species of parasitic dinoflagellates have been classified as members of the Blastodiniphyceae or Syndiniophyceae, with only a few genera placed among the Dinophyceae (see Coats 1999 for review). Recent work, however, has demonstrated that the Blastodiniphyceae is an artificial assemblage, with several of its members now distributed among the Dinophyceae (Gómez, Moreira, and López-García 2009; Landsberg et al. 1994; Levy et al. 2007; Litaker et al. 1999; Saldarriaga et al. 2001; Skovgaard and Salomonsen 2009; Skovgaard, Massana, and Saiz 2007). As in these reports, our phylogenies placed *Amyloodinium*, *Blastodinium*, *Chytridinium*, *Dissodinium*, and *Piscinoodinium* within the Dinophyceae, well removed from the syndinian genera *Syndinium*, *Hematodinium*, *Amoebophrya*, *Duboscquella*, and *Ichthyodinium*. Our results also placed *T. acutus* and *D. collini* (previously classified as a syndinean) deep within the Dinophyceae and nested among thecate dinoflagellates, establishing that neither species belongs to the Syndiniophyceae.

The rDNA sequences of *T acutus* and *D. collini* differed by 3.5% in the SSU rDNA and by 9.1% across the SSU, ITS1, 5.8S region, ITS2, and partial LSU rDNA region, supporting morphological criteria for separation at the species level. Phylogenetic analyses using SSU rDNA sequences linked *T. acutus* to a well-supported clade containing genera typically assigned to the Pfiesteriaceae (Mason et al. 2007; Steidinger et al. 2006) and closely associated *D. collini* with *Scrippsiella*; including the type species *S. sweeneyae*.

Expanding our phylogenies to consider a longer region of the rDNA region (i.e. SSU through partial LSU rDNA region) provided strong support for an affiliation between *D. collini* and *S. trochoidea*, suggesting that the two species may be congeneric. That notion was also supported by the gross similarity in rDNA sequences of *D. collini* and *S. trochoidea*, as the two differed by $<1\%$ in the SSU rDNA and by only 2.4% across the SSU through partial LSU rDNA region. Certainly, additional study of *D. collini* life-history stages, including assessment of plate tabulation in the dinospore stage, is needed before its taxonomic status can be adequately assessed.

Even our SSU–LSU phylogenies failed to clearly define associations between *T. acutus* and closely related Dinophyceae, although two of our three tree building methods (i.e. ML and Bayesian inference) placed it as a sister lineage to the *D. collini–S. trochoidea* clade and basal to clades predominantly composed of lightly thecate Dinophyceae. Thus, we refrain from assigning *T. acutus* to a family of dinoflagellates, opting instead to include it in the Dinophyceae and provisionally within the subclass Peridiniphycidae, based on phylogenetic analyses and

morphological observations suggesting the presence of delicate thecal plates.

TAXONOMIC SUMMARY

Phylum Dinoflagellata Bütschli, 1885, emend. Fensome et al., 1993
Subphylum Dinokaryota Fensome et al., 1983
Class Dinophyceae Pascher, 1914
Subclass Peridiniphycidae Fensome et al., 1983 (*incertae sedis*)

Tintinnophagus Coats n. g.

Diagnosis. Aplastidic ectoparasites feeding on tintinnid ciliates. Trophont lacks flagella, cingulum, and girdle, feeds myzocytotically on host, and possesses a dinokaryon with chromosomes visible in vivo or after staining. Reproduces by palintomic sporogenesis to form numerous biflagellate dinospores with clearly defined cingulum and sulcus. Outer membrane or cyst wall present during palintomy; absent or inconspicuous in trophont. Dinospores with condensed chromosomes.

Type species. *Tintinnophagus acutus* Coats, 2010

Type host. *Tintinnopsis cylindrica* Daday, 1887

Epithet. Genus name is derived from type host genus, *Tintinnopsis*, and the Greek phaein (-phagos) meaning eat (-eating) and is Latinized in the masculine to imply tintinnid eater.

Tintinnophagus acutus Coats n. sp.

Diagnosis. Dinospore 13–16 by 9–12 μm with rigid form, sharply pointed episome terminating in a cylindrical ''knob,'' and a conspicuous yellow to orange cylindrical or crescent-shaped eyespot at base of flagella. Large, ovoid to reneform nucleus positioned posteriorly in cell. Cingulum offset by one-half its width at union with sulcus. Trophont variable in dimension depending on age, with nucleus and nucleolus increasing in size with cell growth.

Type Host. *Tintinnopsis cylindrica* Daday, 1887

Type habitat. The mesohaline portion of Chesapeake Bay, a moderately stratified estuary bordered by the states of Maryland and Virginia, USA.

Type locality. Rhode River, MD, USA (38°53.14′N; 76°32.50′W).

Type material. Hapantotypes, slides with protargol-impregnated *T. cylindrica* infected by *T. acutus*, have been deposited in the International Protozoan Type Slide Collection, National Museum of Natural History, Washington, DC, USA and given the following registration numbers: 1142429 [IZ] and 1142430 [IZ].

Epithet. Species name is the Latin *acutus* meaning pointed and is used to reflect the sharp convergence of the episome at the cell apex.

Gene sequence. The SSU–LSU rDNA sequence is deposited as GenBank Accession No. HM483397.

ACKNOWLEDGMENTS

This work was funded in part by a National Science Foundation, Assembling the Tree of Life grant to C.F.D, D.W.C., and colleagues (EF-06299624) and a NSF Biological Oceanography award OCE-8911316 to D.W.C. Support on a Smithsonian Postdoctoral Fellowship enabled Sunju Kim to participate in the project. Collection and processing of sample in Villefranche-sur-Mer were made possible through the hospitality of Dr. John R. Dolan, Laboratoire d'Océanographie de Villefranche Station Zoologique, and by logistic support from the ANR-BIODIVERSITE project AQUAPARADOX. We are greatly indebted to Dr. Sabine Agatha, Fachbereich Organismische Biologie, Universität Salzburg for advice on tintinnid taxonomy and to Lois Reid for illustrations.

LITERATURE CITED

Agatha, S. & Riedel-Lorjé, J. C. 2006. Redescription of *Tintinnopsis cylindrica* Daday, 1887 (Ciliophora: Spirotricha) and unification of tintinnid terminology. *Acta Protozool.*, **45**:137–151.

Akselman, R. & Santinelli, N. 1989. Observaciones sobre dinoflagelados parasitos en el litoral Atlantico sudoccidental. *Physis, B. Aires, Sec. A*, **47**:43–44.

Ball, G. H. 1969. Organisms living on and in protozoa. *In*: Chen, T. T. (ed.), Research in Protozoology. Vol. 3. Pergamon Press Ltd., Oxford, 565–718.

Cachon, J. 1964. Contribution à l'étude des péridiniens parasites. Cytologie, cycles évolutifs. *Ann. Sci. Nat. Zool.*, **6**:1–158.

Cachon, J. & Cachon, M. 1987. Parasitic dinoflagellates. *In*: Taylor, F. J. R. (ed.), The Biology of Dinoflagellates. Blackwell Science Publication, Oxford. p. 571–610.

Castresana, J. 2000. Selection of conserved blocks from multiple alignments for their use in phylogenetic analysis. *Mol. Biol. Evol.*, **17**:540–552.

Chatton, É. 1920. Les peridiniens parasites: morphologie, reproduction, ethologie. *Arch. Zool. Exp. Gen.*, **59**:1–475.

Chatton, É. 1952. Classe des Dinoflagellés ou Péridiniens. *In*: Grassé, P.-P. (ed.), Traité de Zoologie. Masson & Cie, Paris. p. 309–390.

Coats, D. W. 1988. *Duboscquella cachoni* sp. nov., a parasitic dinoflagellate lethal to its tintinnine host *Eutintinnus pectinis*. *J. Protozool.*, **35**:607–617.

Coats, D. W. 1999. Parasitic life styles of marine dinoflagellates. *J. Eukaryot. Microbiol.*, **46**:402–409.

Coats, D. W. & Heinbokel, J. F. 1982. A study of reproduction and other life cycle phenomena in planktonic protists using an acridine orange fluorescence technique. *Mar. Biol.*, **67**:71–79.

Coats, D. W. & Park, M. G. 2002. Parasitism of photosynthetic dinoflagellates by three strains of *Amoebophrya* (Dinophyta): parasite survival, infectivity, generation time, and host specificity. *J. Phycol.*, **38**:520–528.

Coats, D. W., Bockstahler, K. R., Berg, G. M. & Sniezek, J. H. 1994. Dinoflagellate infections of *Favella panamensis* from two North American estuaries. *Mar. Biol.*, **119**:105–113.

Dider, E. S., Orensterin, J. M., Aldras, A., Bertucci, D., Rogers, L. & Janney, F. A. 1995. Comparison of three staining methods for detecting microsporidia in fluids. *J. Clin. Microbiol.*, **33**:3138–3145.

Doyle, J. J. & Doyle, J. L. 1987. A rapid DNA isolation procedure for small quantities of fresh leaf tissue, *Phytochem. Bulletin*, **19**:11–15.

Duboscq, O. & Collin, B. 1910. Sur la reproduction sexuée d'un protiste parasite des tintinnides. *Comptes Rendus Hebdomadaires des Séances de l'Académie des Sciences, Paris*, **151**:340–341.

Entz, G. Jr. 1909. Studien uber Organisation und biologie der Tintinniden. *Arch. Protistenk.*, **15**:93–226.

Eschbach, E., Reckermann, M., John, U. & Medlin, L. K. 2001. A simple and highly efficient fixation method for *Chrysochromulina polylepis* (Prymnesiophytes) for analytical flow cytometry. *Cytometry*, **44**:126–132.

Fensome, R. A., Taylor, F. J. R., Norris, G., Sargeant, W. A. S., Wharton, D. I. & William, G. L. 1993. A Classification of Living and Fossil Dinoflagellates. Micropaleontology, Special Publication no. 7. Sheridan Press, Hanover. 351p.

Fritz, L. & Triemer, R. E. 1985. A rapid simple technique utilizing calcofluor white m2r for the visualization of dinoflagellate thecal plates. *J. Phycol.*, **21**:662–664.

Glasgow, H. B., Burkholder, J. M., Morton, S. L. & Springer, J. 2001. A second species of ichthyotoxic *Pfiesteria* (Dinamoebales, Dinophyceae). *Phycologia*, **40**:234–245.

Gómez, F., Moreira, D. & López-García, P. 2009. Life cycle and molecular phylogeny of the dinoflagellates *Chytriodinium* and *Dissodinium*, ectoparasites of copepod eggs. *Eur. J. Protist.*, **45**:260–270.

Guillard, R. R. L. & Ryther, J. H. 1962. Studies on marine planktonic diatoms. I. *Cyclotella nana* Hustedt and *Detonula confervacea* (Cleve) Gran. *Can. J. Microbiol.*, **8**:229–239.

Guillou, L., Viprey, M., Chambouvet, A., Welsh, R. M., Kirkham, A. R., Massana, R., Scanlan, D. J. & Worden, A. Z. 2008. Widespread occurrence and genetic diversity of marine parasitoids belonging to *Syndiniales* (*Alveolata*). *Mol. Micro. Ecol.*, **10**:3349–3365.

Hada, Y. 1932. Description of two new neritic Tintinnoinea, *Tintinnopsis japonica* and *Tps. kofoidi* with a brief note on an unicellular organisms parasitic on the latter *Zool. Inst., Fac. Sci. Hokkaido Imp. Univ., Sapporo*, **30**:209–212.

Haeckel, E. 1873. Ueber einige neue pelagische Infusorien. *Jenaische Zeitschrift fur Medizin und Naturwissenschaft*, **7**:561–567.
Handy, S., Bachvaroff, T., Timme, R., Coats, D. W., Kim, S. & Delwiche, C. 2009. Phylogeny of the Dinophysiaceae (Dinophyceae, Dinophysiales) based on rDNA genes. *J. Phycol.*, **45**:1163–1174.
Hansen, G., Daugbjerg, N. & Henriksen, P. 2007. *Baldinia anauniensis* gen. et sp. nov.: a 'new' dinoflagellate from Lake Tovel, N. Italy. *Phycologia*, **46**:86–108.
Harada, A., Ohtsuka, S. & Horiguchi, T. 2007. Species of the parasitic genus *Duboscquella* are members of the enigmatic marine alveolate Group I. *Protist*, **158**:337–347.
Huelsenbeck, J. P. & Ronquist, F. 2001. MrBayes: Bayesian inference of phylogenetic trees. *Bioinformatics*, **17**:754–755.
Laackmann, H. 1906. Ungeschlechtliche und geschlechtliche Fortpflanzung der Tintinnen. *Zoologischer Anzeiger*, **30**:440–443.
Laackmann, H. 1908. Ungeschlechtliche und geschlechtliche Fortpflanzung der Tintinnen. *Wissenschaftliche Meeresuntersuchung, N. F.*, **10**:13–38.
Landsberg, J. H., Steidinger, K. A., Blakesley, B. A. & Zondervan, R. L. 1994. Scanning electron microscope study of dinospores of *Amyloodinium* cf. *ocellatum*, a pathogenic dinoflagellate parasite of marine fish, and comments on its relationship to the peridiniales. *Dis. Aquat. Org.*, **20**:23–32.
Levy, M. G., Litaker, R. W., Goldstein, R. J., Dykstra, M. J., Vandersea, M. W. & Noga, E. J. 2007. *Piscinoodinium*, a fish-ectoparasitc dinoflagellate, is a member of the class Dinophyceae, subclass Gymnodiniphycidae: convergent evolution with *Amyloodinium*. *J. Parasitol.*, **93**:1006–1015.
Litaker, R. W., Tester, P. A., Colorni, A., Levy, M. G. & Noga, E. J. 1999. The phylogenetic relationship of *Pfiesteria piscicida*, cryptoperidiniopsoid sp., *Amyloodinium ocellatum* and a *Pfiesteria*-like dinoflagellate to other dinoflagellates and apicomplexans. *J. Phycol.*, **35**:1379–1389.
Lohmann, H. 1908. Untersuchung zur Feststellung des vollständigen Gehaltes des Meeres an Plankton. *Wissenschaftliche Meeresuntersuchung, N. F.*, **10**:129–370.
Maddison, W. P. & Maddison, D. R. 2002. MacClade: Analysis of Phylogeny and Character Evolution. Sinauer, Sunderland, MA.
Mason, P. L., Vogelbein, W. K., Haas, L. W. & Shields, J. D. 2003. An improved stripping technique for lightly armored dinoflagellates. *J. Phycol.*, **39**:253–258.
Mason, P. L., Litaker, R. W., Jeong, H. J., Ha, J. H., Reece, K. S., Stokes, N. A., Park, J. Y., Steidinger, K. A., Vandersea, M. W., Kibler, S., Tester, P. A. & Vogelbein, W. K. 2007. Description of a new genus of *Pfiesteria*-like dinoflagellate *Luciella* gen. nov. (Dinophyceae), including two new species: *Luciella masanensis* sp. nov. and *Luciella atlantis* sp. nov. *J. Phycol.*, **43**:799–810.
Moestrup, Ø., Hansen, G. & Daugbjerg, N. 2008. Studies on woloszynskioid dinoflagellates III: on the ultrastructure and phylogeny of *Borghiella dodgei* gen. et sp. nov., a cold-water species from Lake Tovel, N. Italy, and on *B. tenuissima* comb. nov. (syn. *Woloszynskia tenuissima*). *Phycologia*, **47**:54–78.
Montagnes, D. J. S. & Lynn, D. H. 1993. A quantitative protargol stain (QPS) for ciliates and other protists. *In*: Kemp, P. F., Sherr, B. F., Sherr, E. B. & Cole, J. J. (ed.), Handbook of Methods in Aquatic Microbial Ecology. Lewis Publishers, Boca Raton. p. 229–240.
Morgan, D. R. & Soltis, D. E. 1995. Phylogenetic relationships among members of Saxifragaceae *sensu lato* based on *rbcL* sequences data. *Ann. Missouri Bot. Gar.*, **82**:208–234.
Palacios, L. & Marín, L. 2008. Enzymatic permeabilization of the thecate dinoflagellate *Alexandrium minutum* (Dinophyceae) yields detection of intracellularly associated bacteria via catalyzed reporter deposition-fluorescence in situ hybridization. *Appl. Environ. Microbiol.*, **74**:2244–2247.
Parrow, M. W., Elbrächter, M., Krause, M. K., Burkholder, J. M., Deamer, N. J., Htyte, N. & Allen, E. A. 2006. The taxonomy and growth of a *Crypthecodinium* species (Dinophyceae) isolated from a brackish-water fish aquarium. *African J. Mar. Sci.*, **28**:185–191.
Posada, D. & Crandall, K. A. 1998. Modeltest: testing the model of DNA substitution. *Bioinformatics*, **14**:817–818.
Saldarriaga, J. F., Taylor, F. J. R., Keeling, P. J. & Cavalier-Smith, T. 2001. Dinoflagellate nuclear SSU r-RNA phylogeny suggests multiple plastid losses and replacements. *J. Mol. Evol.*, **53**:204–213.
Skovgaard, A. & Salomonsen, X. M. 2009. *Blastodinium galatheanum* sp. nov. (Dinophyceae) a parasite of the planktonic copepod *Acartia negligens* (Crustacea, Calanoida) in the central Atlantic Ocean. *Eur. J. Phycol.*, **44**:425–438.
Skovgaard, A., Massana, R. & Saiz, E. 2007. Parasitic species of the genus *Blastodinium* (Blastodiniphyceae) are peridinioid dinoflagellates. *J. Phycol.*, **43**:553–560.
Skovgaard, A., Menese, I. & Angélico, M. M. 2009. Identifying the lethal fish egg parasite *Ichthyodinium chabelardi* as a member of Marine Alveolate Group I. *Environ. Microbiol.*, **11**:2030–2041.
Skovgaard, A., Massana, R., Balagué, V. & Saiz, E. 2005. Phylogenetic position of the copepod-infesting parasite *Syndinium turbo* (Dinoflagellata, Syndinea). *Protist*, **156**:413–423.
Stamatakis, A. 2006. RAxML-VI-HPC: maximum likelihood-based phylogenetic analysis with thousands of taxa and mixed models. *Bioinformatics*, **22**:2688–2690.
Steidinger, K. A., Landsberg, J. H., Truby, E. W. & Blakesley, B. A. 1996. The use of scanning electron microscopy in identifying small ''gymnodinoid'' dinoflagellates. *Nova Hedwigia*, **112**:415–422.
Steidinger, K. A., Landsberg, J. H., Mason, P. L., Vogelbein, W. K., Tester, P. A. & Litaker, R. W. 2006. *Cryptoperidiniosis brodyi* gen. et sp. nov. (Dinophyceae), a small lightly armored dinoflagellate in the Pfiesteriaceae. *J. Phycol.*, **42**:951–961.
Swofford, D. L., Olsen, G. J., Waddell, P. J. & Hillis, D. M. 2002. PAUP*. Phylogenetic Analysis Using Parsimony (*and Other Methods). Version 4. Sinauer Associates, Sunderland.
Thompson, J. D., Gibson, T. J., Plewniak, F., Jeanmougin, F. & Higgins, D. G. 1997. The ClustalX windows interface: flexible strategies for multiple sequence alignment aided by quality analysis tools. *Nucleic Acids Res.*, **24**:4876–4882.

SUPPORTING INFORMATION

Additional Supporting Information may be found in the online version of this article:

Table S1. Taxa and GenBank accession numbers used to infer phylogenetic trees.

Please note: Wiley-Blackwell are not responsible for the content or functionality of any supporting materials supplied by the authors. Any queries (other than missing material) should be directed to the corresponding author for the article.

Received: 04/05/10, 07/12/10; accepted: 07/13/10